TABLE IV. List of Genes Upregulated Greater Than Twofold in HFD

Gene symbol	Gene	Gene ID	Function	Mean fold change
TMEM22	Transmembrane protein 22	NM_025246	Unknown	8.04
MAT1A	**Methionine adenosyltransferase I, alpha**	**BC018359**	**Nucleotide binding**	**7.36**
OR2G2	Olfactory receptor, family 2, subfamily G, member 2	NM_001001915	Signal transducer activity	6.70
HBB	Hemoglobin, delta	NM_000519	Transporter activity	5.88
O8D4_HUMAN	Olfactory receptor, family 8, subfamily D, member 4	NM_001005197	Signal transducer activity	5.68
CYP21A2	Cytochrome P450, family 21, subfamily A, polypeptide 2	CD013987	Oxygen binding	5.52
NP_659484	Oxidored-nitro domain-containing protein	NM_206837	Unknown	5.38
C10orf79	Chromosome 10 open reading frame 79	BC071565	Unknown	5.33
C18orf26	Chromosome 18 open reading frame 26	AK096425	Metal ion binding	5.32
HBB	Hemoglobin, beta	BM811415	Transporter activity	5.07
PCNX	Pecanex homolog	AF233450	Unknown	5.06
WDR17	WD repeat domain 17	BX648508	Unknown	4.88
ACAA1	Acetyl-Coenzyme A acyltransferase 1	NM_001607	C-acyltransferase activity	4.68
SLC5A6	**Sodium-dependent vitamin transporter**	**AL096737**	**Binding**	**4.67**
HYOU1	**Hypoxia up-regulated 1**	**U65785**	**Protein binding**	**4.63**
MMP16	Matrix metalloproteinase 16	D83646	Metal ion binding	4.46
RPS6KA6	Ribosomal protein S6 kinase, 90 kDa, polypeptide 6	AF184965	Neuroscience, binding	4.46
GPR8	G protein-coupled receptor 8	BC067483	Binding	4.41
B4GALT4	UDP-Gal:betaGlcNAc beta 1,4-galactosyltransferase, polypeptide 4	AK001006	Catalytic activity	4.38
NSUN2	NOL1/NOP2/Sun domain family, member 2	NM_017755	Unknown	4.29
TNFRSF12A	**Tumor necrosis factor receptor superfamily, member 12A**	**AB035480**	**Extracellular matrix and adhesion melecules, binding**	**3.98**
HBA1	Hemoglobin, alpha 1	BQ709225	Binding	3.89
SKIP_HUMAN	Skeletal muscle and kidney enriched inositol phosphatase	CR623148	Lipid phosphatase activity	3.82
WISP1	**WNT1 inducible signaling pathway protein 1**	**AF100779**	**Signal transduction, growth factor binding**	**3.80**
NP_660318	Kinesin light chain 2-like	NM_177417	Motor activity	3.72
ALAS2	Aminolevulinate, delta-, synthase 2	BC030230	Signal transduction, transferase activity	3.68
JTB	**Jumping translocation breakpoint**	**AF131797**	**Cancer**	**3.66**
NP_690005	Hypothetical protein FLJ25084	AK055994	Transferase activity	3.63
COCH	Coagulation factor C homolog, cochlin	AK123362	Unknown	3.61
MCMDC1	Minichromosome maintenance deficient domain containing 1	BX649114	Catalytic activity	3.61
RIMS1	Regulating synaptic membrane exocytosis 1	AF263307	Metal ion binding	3.46
Q86YV5	Hypothetical protein DKFZp761P0423	XM_291277	Binding	3.45

(*Continued*)

TABLE IV. (*Continued*)

Gene symbol	Gene	Gene ID	Function	Mean fold change
IGFIR	**Insulin-like growth factor 1 receptor**	**NM_000875**	**Signal transduction**	**3.43**
P2CE_HUMAN	Likely ortholog of mouse protein phosphatase 2C eta	AK056894	Cation binding	3.43
CCL5	Chemokine (C–C motif) ligand 5	NM_002985	Signal transduction, cytokine activity	3.42
NP_981947	Similar to CG10671-like	NM_203402	Unknown	3.31
NRG1	Neuregulin 1	NM_013958	Receptor tyrosine kinase binding	3.30
NAGK	N-acetylglucosamine kinase	AK001812	Carbohydrate kinase activity	3.25
HPS5	Hermansky–Pudlak syndrome 5	BC033640	Unknown	3.21
C1QTNF6	C1q and tumor necrosis factor related protein 6	AK128125	Unknown	3.19
NP_056248	Hepatocellularcarcinoma-associated antigen HCA557a	AL050100	Unknown	3.06
NP_919266	Hypothetical protein LOC153684	AK123995	Unknown	3.06
HERC4	Hect domain and RLD 4	AK026808	Catalytic activity	3.04
NLGN4X	Neuroligin 4, X-linked	NM_181332	Binding	3.03
ASB15	Ankyrin repeat and SOCS box-containing 15	AK125360	Unknown	3.00
HBQ1	Hemoglobin, theta 1	BM479599	Transporter activity	2.96
MPP4	Membrane protein, palmitoylated 4	BX647162	Binding	2.84
ACP6	Acid phosphatase 6, lysophosphatidic	AB031478	Catalytic activity	2.79
ADAMTS9	A disintegrin-like and metalloprotease with thrombospondin type 1 motif, 9	NM_182920	Metal ion binding	2.67
PPM1F	Protein phosphatase 1F	AK126377	Cation binding	2.64
OR7G3	Olfactory receptor, family 7, subfamily G, member 3	NM_001001958	Signal transducer activity	2.63
MRPL2	Mitochondrial ribosomal protein L2	NM_015950	Structural molecule activity	2.58
SDSL	Serine dehydratase-like	BC009849	Catalytic activity	2.54
PMP22	**Peripheral myelin protein 22**	**D11428**	**Signal transduction**	**2.52**
ARFIP2	Arfaptin 2	AK026390	Nucleotide binding	2.45
GPNMB	Glycoprotein (transmembrane) nmb	X76534	Unknown	2.44
NP_056147	KIAA1068 protein	AB028991	Unknown	2.43
RASSF3	Ras association (RalGDS/AF-6) domain family 3	AY217662	Binding	2.41
NP_060712	Hypothetical protein FLJ10847	BC010661	Carrier activity	2.33
APBB1	Amyloid beta (A4) precursor protein-binding, family B, member 1	L77864	Enzyme binding	2.32
HAPLN1	Hyaluronan and proteoglycan link protein 1	U43328	Pattern binding	2.28
O43162	Pecanex-like 2	AB007895	Unknown	2.26
CDC25C	Cell division cycle 25C	NM_022809	Catalytic activity	2.24
SH3BGRL2	SH3 domain binding glutamic acid-rich protein like 2	AF340151	Unknown	2.10

and 225 down-regulated genes with <0.66-fold difference on the HFD xenograft. Furthermore, 64 genes were found to be up-regulated more than 2.0-fold and 14 genes were down-regulated more than 0.5-fold by two independent microarray experiments. Many genes related to apoptosis, cancer and the cell cycle were shown to change their expression levels under HFD. The expression levels of all the candidate genes were not confirmed in this study, and it is difficult to clarify the relationship and interaction among all these genes.

Among the 12 genes selected for further validation study, the major gene of interest up-regulated by HFD is *IGF-IR*. This was confirmed by markedly increased

TABLE V. List of Genes Downregulated Greater Than Twofold in HFD

Gene symbol	Gene	Gene ID	Function	Mean fold change
LPL	**Lipoprotein lipase**	**M15856**	**Pattern binding**	**0.23**
TPM1	**Tropomyosin 1**	**NM_000366**	**Structural constituent of cytoskeleton**	**0.24**
CTSS	Cathepsin S	M90696	Endopeptidase activity	0.3
NP_653271	Hypothetical protein FLJ25179	AK057908	Enzyme regulator activity	0.3
LYZ	Lysozyme	AK130149	Catalytic activity	0.33
GAPDS	Glyceraldehyde-3-phosphate dehydrogenase, spermatogenic	AJ005371	Catalytic activity	0.38
PAX5	Paired box gene 5	M96944	Signal transduction, binding	0.39
LGALS1	**Galectin 1**	**NM_002305**	**Binding**	**0.41**
STAT1	Signal transducer and activator of transcription 1, 91 kDa	CR749636	Receptor signaling protein activity	0.42
DCN	Decorin	NM_133505	Unknown	0.42
QKI	Quaking homolog	AB067801	Binding	0.42
UBC1_HUMAN	Huntingtin interacting protein 2	CR605719	Ligase activity	0.45
GNAI2	Guanine nucleotide binding protein, alpha inhibiting activity polypeptide 2	AK126708	Catalitic activity	0.45
OR5V1	Olfactory receptor, family 5, subfamily V, member 1	AJ459859	Signal transduction	0.46
ID2	**Inhibitor of DNA binding 2, dominant negative helix-loop-helix protein**	**CR623038**	**Signal transduction**	**0.49**

expressions in both mRNA and protein level. The IGF axis has been shown to be involved in the regulation of cellular proliferation, differentiation and apoptosis of PCa cells [20]. In the case-control study of PCa, the plasma IGF-I level was significantly higher in PCa patients than controls [20]. One study, which demonstrated the association between the serum IGF-I level and diet, showed that the serum level of IGF-I was positively associated with the consumption of red meats, fats, and oils [21]. Interestingly, linoleic acid and oleic acid amplified glucose-stimulated insulin secretion, known to stimulate the hepatic production of IGF-I [22], and enhanced the growth-promoting effect of IGF-I in smooth muscle isolated from diabetic pigs [23,24]. In these studies, the IGF axis may play an important role in the development of PCa cells through unsaturated fatty acids. Furthermore, in an LAPC-4 xenograft study, Ngo et al. found that mice with LFD had a significantly lower expression level of serum insulin, tumor IGF-I mRNA expression, and tumor IGFBP-2 immunostaining, and higher levels of serum IGFBP-1 compared to mice with LFD. They presumed that the IGF axis may play a role in LFD-induced reduction in PCa growth [12].

IGF-IR was demonstrated to be overexpressed in cancer cells and tumors in vivo compared to normal cell lines and tumors by both experimental and clinical studies [25,26]. Studies on PCa have shown that an increase in IGF-IR expression was associated with the growth of PCa cells, and antisense-mediated inhibition of the *IGF-IR* expression suppressed in vivo tumor growth and prevented prostate cell invasion [17,27–29]. The association between dietary factors and IGF-IR has been less demonstrated; however, dietary administration of corticosterone, which is usually increased during energy restriction, has been shown to reduce not only the incidence of carcinoma but also the protein expression levels of IGF-IR [30]. On the other hand, a recent study showed that androgens upregulate the expression of IGF-IR in PCa cells [31]. Since androgen levels may be modified by HFD or LFD [32], the increased expression of IGF-IR may be due to the change in androgen levels caused by HFD. Furthermore, the activation of IGF-IR was suggested to be reflected by circulating levels of IGF-I and its binding proteins as well as by paracrine/autocrine IGF effects [33]. Although IGF-IR binds IGF-I and IGF-II to activate downstream signaling in general, the mechanisms of ligand-receptor activation are largely unknown [34]. In this study, we found no difference in the mRNA expression level of IGF-I between the HFD and the xenograft in the microarray, and the serum IGF-I level was not calculated. Further studies are warranted to delineate the precise direct or indirect mechanisms underlying the enhanced expression of IGF-IR. Furthermore, it would be interesting to know whether

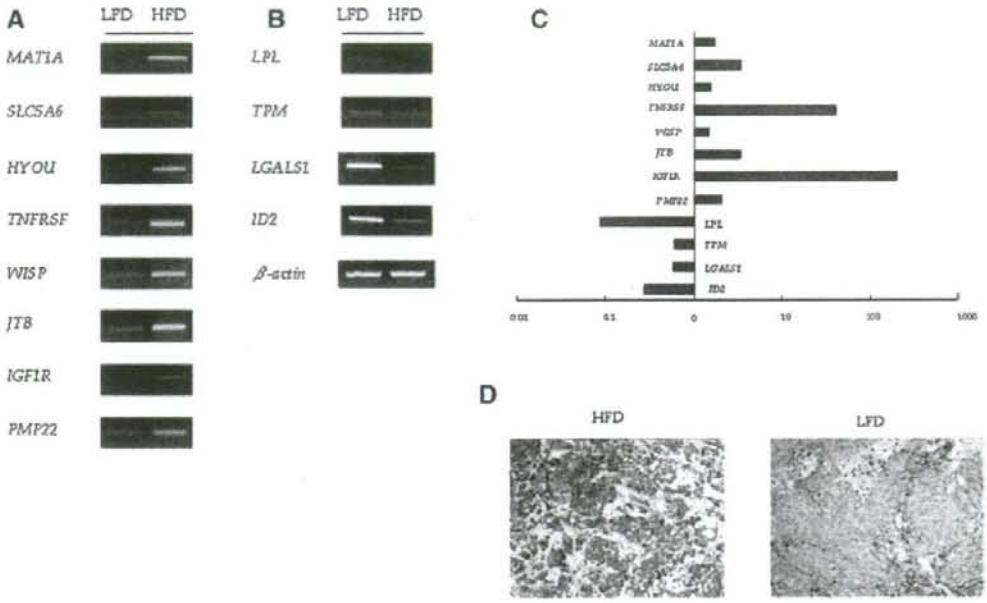

Fig. 3. Validation of microarray results. **A**,**B**: Validation of microarray results by semiquantitative RT-PCR analysis using distinct RNAs from LNCaP xenografts fed with HFD or LFD. A: List of genes with up-regulated expression in the HFD xenograft by microarray analysis. B: List of genes with down-regulated expression in HFD xenograft. Beta-actin expression is shown as an internal control. **C**: Comparison of the relative expression ratios of target genes using quantitative real-time PCR. The values are presented on a logarithmic scale. **D**: Immunohistochemical staining of IGF-IR in xenograft tumor tissues from HFD and LFD mice. The left panel of HFD shows striking staining in the cytoplasm as well as the membrane of tumor cells, while the **right panel** of LFD shows weak staining.

the administration of IGF-IR-specific kinase inhibitors, such as ADW742 and NVP-AEW541 [35,36], suppresses the enhanced growth of LNCaP xenograft by HFD.

In the present study, there was no statistically significant relationship between IGF-IR immunostaining and BMI in PCa patients, although it is unclear to what extent human tissue might reflect the effect of previous diet consumption. Interestingly, both normal epithelium and PCa cells in specimens from the lowest IGF-IR immunoreactivity group tended to have lower BMI levels. The results suggest that IGF-IR activation under HFD may play a role in the carcinogenesis of normal epithelium in the human prostate. As BMI is a fictitious value, it would be interesting to investigate IGF-IR expression in human PCa and prostate tissues using a different value and/or method to assess the relationship between IGF-IR expression and obesity through high fat intake.

Another up-regulated gene of interest is *TNFRSF12A*, which is also called a TNF-like weak inducer of apoptosis receptor (TWEAKR). It has been suggested that TWEAK/TWEAKR may promote tumor cell growth in several kinds of human cancer. Kawakita et al. [37] reported that hepatocellular carcinoma cell lines constantly secreted TWEAK, which can promote proliferation in an autocrine manner and induce angiogenesis in vitro. Activation of the TWEAK/TWEAKR system has been shown to enhance resistance to apoptosis in glioma cancer cells via activation of the NF-kB pathway and enhanced BCL-X1/BCL-W expression [38]. The present study is the first to show that LNCaP PCa cells express TWEAKR, and it remains to be known whether TWEAKR is expressed in other PCa cell lines or human PCa tissues in vivo. Further studies are warranted to elucidate the role of the TWEAK/TWEAKR system in the progression of PCa, especially in relation to HFD.

On the other hand, the mRNA expression level of *LPL* was significantly lower in the HFD xenograft. LPL has been shown to play a crucial role in fat metabolism, and LPL overexpression may protect against diet-induced hypertriglyceridemia as well as hypercholesterolemia [39]. Recently, we have demonstrated the association between the *LPL* single nucleotide polymorphism and susceptibility to PCa [40]. In gastric and colon cancer studies, LPL activity in the plasma of patients with metastasis was significantly reduced

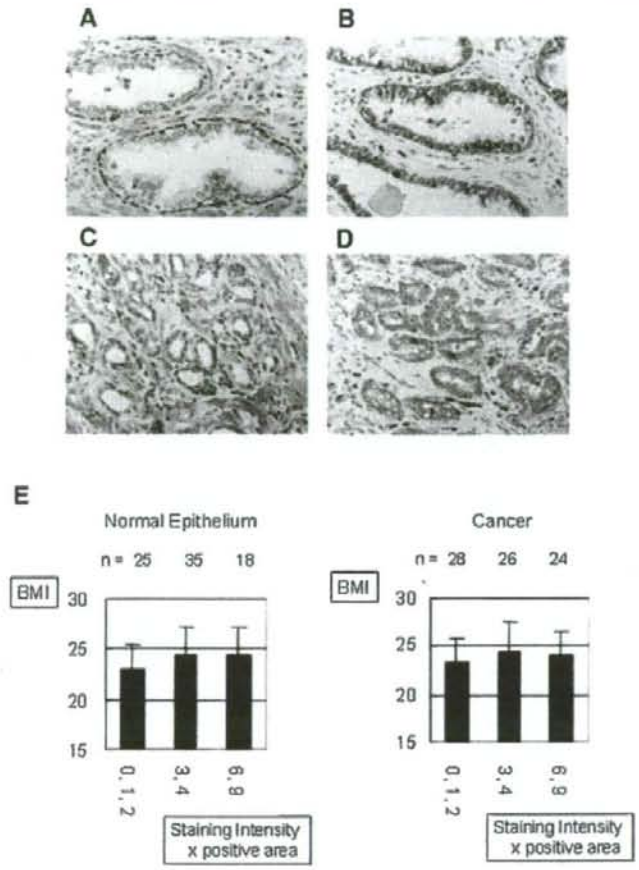

Fig. 4. IGF-IR staining and BMI in human prostate tissue. **A**: Absent IGF-IR expression (total staining score, 0) in normal epithelial region. **B**: Strong IGF-IR expression (total staining score, 9) in normal epithelial region. **C**: Absent IGF-IR expression in PCa cells. **D**: Strong IGF-IR expression in almost all PCa cells. **E**: The relationship between the total immunoreactivity score in normal epithelium or in PCa cells in radical prostatectomy specimen and corresponding patient's BMI. Note that patients with the lowest IGF-IR immunostaining group had the lowest BMI both in the normal epithelium and PCa.

compared to the non-metastatic group [41]. Interestingly, human lung cancer cells have been shown to secrete an unknown LPL-inhibiting factor, thus promoting cancer cahexia [42]. The down regulation of LPL has been shown in breast cancer patients, and LPL activity was suggested to be further suppressed by an aromatase inhibitor, tamoxifen [43]. It remains to be known whether the downregulation of LPL might have a causative role in enhanced growth under HFD in this LNCaP xenograft model, or it might be a mere reflection of systematic metabolic modification under HFD.

Differential expressed genes in our study included genes classified in apoptosis, cancer, cell cycle, cell and development biology, extracellular matrix and adhesion molecular, biomarker, cytokine and inflammatory responses, and signal transduction in the Gene Ontology category. Furthermore, *SLC5A6*, *JTB*, *PMP22*, and *ID2*, had more than a 2-fold difference in expression level between HFD and LFD groups on both microarray and quantitative RT-PCR analyses. In particular, ID2 is known to be associated with carcinogenesis, and to be strongly down-regulated in aggressive melanoma tumors [44]. Although we need to confirm these mRNA expression levels using more samples and to validate the expression level of protein, these genes may have the potential to affect the development of PCa complexly. In addition, our microarray analyses were limited to only one pair of xenograft although the significant results were confirmed by other batches of

RNAs from distinct xenografts. Therefore, further extensive microarray analyses may be required to delineate the precise whole gene expression profiles associated with HFD. Furthermore, since our model is based on only LNCaP cancer cell xenografts, it would be interesting to know if identical mRNA expression alterations are found in the normal prostate epithelium after HFD.

CONCLUSIONS

The growth of the LNCaP xenograft was enhanced by HFD with an elevated level of serum PSA in athymic nude mice. Oligonucleotide microarray analysis revealed a substantial number of candidate up- and/or down-regulated genes associated with HFD in the LNCaP xenograft, and provided first-step data for the further clarification of molecular mechanisms underlying the enhanced growth of PCa cells under HFD. Of the HFD-associated candidate genes, we validated eight up-regulated genes and four down-regulated genes by quantitative RT-PCR analyses. Of the 12 genes, the expression of IGF-IR mRNA and protein was shown to be greatly enhanced under HFD. Because of the importance of the IGF pathway in the development and progression of PCa in general, further studies are warranted to elucidate the role of the IGF-I system in the enhanced growth of PCa cells under HFD. Furthermore, clarification of the roles of other differentially expressed genes may reveal not the molecular mechanisms of PCa progression but also new therapeutic and preventive targets.

ACKNOWLEDGMENTS

We greatly thank Yoshiko Shibata, Yukiko Sugiyama and Yoko Mitobe for technical assistance. This work was supported by a Grant-in-Aid for Scientific Research by the Japan Society for the Promotion of Science (17591678).

REFERENCES

1. Jemal A, Murray T, Ward E, Samuels A, Tiwari RC, Ghafoor A, Feuer EJ, Thun MJ. Cancer statistics, 2005. CA Cancer J Clin 2005;55(1):10–30.
2. Watanabe M, Nakayama T, Shiraishi T, Stemmermann GN, Yatani R. Comparative studies of prostate cancer in Japan versus the United States. A review. Urol Oncol 2000;5(6):274–283.
3. Breslow N, Chan CW, Dhom G, Drury RA, Franks LM, Gellei B, Lee YS, Lundberg S, Sparke B, Sternby NH, Tulinius H. Latent carcinoma of prostate at autopsy in seven areas. The International Agency for Research on Cancer, Lyons, France. Int J Cancer 1977;20(5):680–688.
4. Shimizu H, Ross RK, Bernstein L, Yatani R, Henderson BE, Mack TM. Cancers of the prostate and breast among Japanese and white immigrants in Los Angeles County. Br J Cancer 1991; 63(6):963–966.
5. Wakai K. Descriptive epidemiology of prostate cancer in Japan and Western countries. Nippon Rinsho 2005;63(2):207–212.
6. Ornish D, Weidner G, Fair WR, Marlin R, Pettengill EB, Raisin CJ, Dunn-Emke S, Crutchfield L, Jacobs FN, Barnard RJ, Aronson WJ, McCormac P, McKnight DJ, Fein JD, Dnistrian AM, Weinstein J, Ngo TH, Mendell NR, Carroll PR. Intensive lifestyle changes may affect the progression of prostate cancer. J Urol 2005;174(3):1065–1069, discussion 1069–1070.
7. Giovannucci E, Rimm EB, Colditz GA, Stampfer MJ, Ascherio A, Chute CC, Willett WC. A prospective study of dietary fat and risk of prostate cancer. J Natl Cancer Inst 1993;85(19):1571–1579.
8. Fair WR, Fleshner NE, Heston W. Cancer of the prostate: A nutritional disease? Urology 1997;50(6):840–848.
9. Connolly JM, Coleman M, Rose DP. Effects of dietary fatty acids on DU145 human prostate cancer cell growth in athymic nude mice. Nutr Cancer 1997;29(2):114–119.
10. Wang Y, Corr JG, Thaler HT, Tao Y, Fair WR, Heston WD. Decreased growth of established human prostate LNCaP tumors in nude mice fed a low-fat diet. J Natl Cancer Inst 1995;87(19): 1456–1462.
11. Chan JM, Gann PH, Giovannucci EL. Role of diet in prostate cancer development and progression. J Clin Oncol 2005;23(32): 8152–8160.
12. Ngo TH, Barnard RJ, Cohen P, Freedland S, Tran C, deGregorio F, Elshimali YI, Heber D, Aronson WJ. Effect of isocaloric low-fat diet on human LAPC-4 prostate cancer xenografts in severe combined immunodeficient mice and the insulin-like growth factor axis. Clin Cancer Res 2003;9(7):2734–2743.
13. Horoszewicz JS, Leong SS, Kawinski E, Karr JP, Rosenthal H, Chu TM, Mirand EA, Murphy GP. LNCaP model of human prostatic carcinoma. Cancer Res 1983;43(4):1809–1818.
14. Gleave M, Hsieh JT, Gao CA, von Eschenbach AC, Chung LW. Acceleration of human prostate cancer growth in vivo by factors produced by prostate and bone fibroblasts. Cancer Res 1991; 51(14):3753–3761.
15. Liao Y, Abel U, Grobholz R, Hermani A, Trojan L, Angel P, Mayer D. Up-regulation of insulin-like growth factor axis components in human primary prostate cancer correlates with tumor grade. Hum Pathol 2005;36(11):1186–1196.
16. Chan JM, Stampfer MJ, Giovannucci E, Gann PH, Ma J, Wilkinson P, Hennekens CH, Pollak M. Plasma insulin-like growth factor-I and prostate cancer risk: A prospective study. Science 1998;279(5350):563–566.
17. Nickerson T, Chang F, Lorimer D, Smeekens SP, Sawyers CL, Pollak M. In vivo progression of LAPC-9 and LNCaP prostate cancer models to androgen independence is associated with increased expression of insulin-like growth factor I (IGF-I) and IGF-I receptor (IGF-IR). Cancer Res 2001;61(16):6276–6280.
18. Bray GA, Popkin BM. Dietary fat intake does affect obesity! Am J Clin Nutr 1998;68(6):1157–1173.
19. Tjandrawinata RR, Dahiya R, Hughes-Fulford M. Induction of cyclo-oxygenase-2 mRNA by prostaglandin E2 in human prostatic carcinoma cells. Br J Cancer 1997;75(8):1111–1118.
20. Clemmons DR, Klibanski A, Underwood LE, McArthur JW, Ridgway EC, Beitins IZ, Van Wyk JJ. Reduction of plasma immunoreactive somatomedin C during fasting in humans. J Clin Endocrinol Metab 1981;53(6):1247–1250.
21. Kaklamani VG, Linos A, Kaklamani E, Markaki I, Koumantaki Y, Mantzoros CS. Dietary fat and carbohydrates are independently associated with circulating insulin-like growth factor 1 and insulin-like growth factor-binding protein 3 concentrations in healthy adults. J Clin Oncol 1999;17(10):3291–3298.

22. Phillips LS, Harp JB, Goldstein S, Klein J, Pao CI. Regulation and action of insulin-like growth factors at the cellular level. Proc Nutr Soc 1990;49(3):451–458.
23. Itoh Y, Kawamata Y, Harada M, Kobayashi M, Fujii R, Fukusumi S, Ogi K, Hosoya M, Tanaka Y, Uejima H, Tanaka H, Maruyama M, Satoh R, Okubo S, Kizawa H, Komatsu H, Matsumura F, Noguchi Y, Shinohara T, Hinuma S, Fujisawa Y, Fujino M. Free fatty acids regulate insulin secretion from pancreatic beta cells through G PR40. Nature 2003;422(6928):173–176.
24. Askari B, Carroll MA, Capparelli M, Kramer F, Gerrity RG, Bornfeldt KE. Oleate and linoleate enhance the growth-promoting effects of insulin-like growth factor-I through a phospholipase D-dependent pathway in arterial smooth muscle cells. J Biol Chem 2002;277(39):36338–36344.
25. All-Ericsson C, Girnita L, Seregard S, Bartolazzi A, Jager MJ, Larsson O. Insulin-like growth factor-1 receptor in uveal melanoma: A predictor for metastatic disease and a potential therapeutic target. Invest Ophthalmol Vis Sci 2002;43(1):1–8.
26. Xie Y, Skytting B, Nilsson G, Brodin B, Larsson O. Expression of insulin-like growth factor-1 receptor in synovial sarcoma: Association with an aggressive phenotype. Cancer Res 1999;59(15): 3588–3591.
27. Cardillo MR, Monti S, Di Silverio F, Gentile V, Sciarra F, Toscano V. Insulin-like growth factor (IGF)-I, IGF-II and IGF type I receptor (IGFR-I) expression in prostatic cancer. Anticancer Res 2003;23(5A):3825–3835.
28. Burfeind P, Chernicky CL, Rininsland F, Ilan J. Antisense RNA to the type I insulin-like growth factor receptor suppresses tumor growth and prevents invasion by rat prostate cancer cells in vivo. Proc Natl Acad Sci USA 1996;93(14):7263–7268.
29. Grzmil M, Hemmerlein B, Thelen P, Schweyer S, Burfeind P. Blockade of the type I IGF receptor expression in human prostate cancer cells inhibits proliferation and invasion, up-regulates IGF binding protein-3, and suppresses MMP-2 expression. J Pathol 2004;202(1):50–59.
30. Zhu Z, Jiang W, Thompson HJ. Mechanisms by which energy restriction inhibits rat mammary carcinogenesis: In vivo effects of corticosterone on cell cycle machinery in mammary carcinomas. Carcinogenesis 2003;24(7):1225–1231.
31. Pandini G, Mineo R, Frasca F, Roberts CT Jr, Marcelli M, Vigneri R, Belfiore A. Androgens up-regulate the insulin-like growth factor-I receptor in prostate cancer cells. Cancer Res 2005;65(5): 1849–1857.
32. Volek JS, Gomez AL, Love DM, Avery NG, Sharman MJ, Kraemer WJ. Effects of a high-fat diet on postabsorptive and postprandial testosterone responses to a fat-rich meal. Metabolism 2001;50(11):1351–1355.
33. Voskuil DW, Vrieling A, van't Veer LJ, Kampman E, Rookus MA. The insulin-like growth factor system in cancer prevention: Potential of dietary intervention strategies. Cancer Epidemiol Biomarkers Prev 2005;14(1):195–203.
34. Bahr C, Groner B. The IGF-1 receptor and its contributions to metastatic tumor growth-novel approaches to the inhibition of IGF-1R function. Growth Factors 2005;23(1):1–14.
35. Mitsiades CS, Mitsiades NS, McMullan CJ, Poulaki V, Shringarpure R, Akiyama M, Hideshima T, Chauhan D, Joseph M, Libermann TA, Garcia-Echeverria C, Pearson MA, Hofmann F, Anderson KC, Kung AL. Inhibition of the insulin-like growth factor receptor-1 tyrosine kinase activity as a therapeutic strategy for multiple myeloma, other hematologic malignancies, and solid tumors. Cancer Cell 2004;5(3):221–230.
36. Martins AS, Mackintosh C, Martin DH, Campos M, Hernandez T, Ordonez JL, de Alava E. Insulin-like growth factor I receptor pathway inhibition by ADW742, alone or in combination with imatinib, doxorubicin, or vincristine, is a novel therapeutic approach in Ewing tumor. Clin Cancer Res 2006;12(11 Pt 1):3532–3540.
37. Kawakita T, Shiraki K, Yamanaka Y, Yamaguchi Y, Saitou Y, Enokimura N, Yamamoto N, Okano H, Sugimoto K, Murata K, Nakano T. Functional expression of TWEAK in human hepatocellular carcinoma: Possible implication in cell proliferation and tumor angiogenesis. Biochem Biophys Res Commun 2004;318(3):726–733.
38. Tran NL, McDonough WS, Savitch BA, Sawyer TF, Winkles JA, Berens ME. The tumor necrosis factor-like weak inducer of apoptosis (TWEAK)-fibroblast growth factor-inducible 14 (Fn14) signaling system regulates glioma cell survival via NFkappaB pathway activation and BCL-XL/BCL-W expression. J Biol Chem 2005;280(5):3483–3492.
39. Shimada M, Shimano H, Gotoda T, Yamamoto K, Kawamura M, Inaba T, Yazaki Y, Yamada N. Overexpression of human lipoprotein lipase in transgenic mice. Resistance to diet-induced hypertriglyceridemia and hypercholesterolemia. J Biol Chem 1994;269(15):11673.
40. Narita S, Tsuchiya N, Wang L, Matsuura S, Ohyama C, Satoh S, Sato K, Ogawa O, Habuchi T, Kato T. Association of lipoprotein lipase gene polymorphism with risk of prostate cancer in a Japanese population. Int J Cancer 2004;112(5):872–876.
41. Nomura K, Noguchi Y, Yoshikawa T, Kondo J. Plasma interleukin-6 is not a mediator of changes in lipoprotein lipase activity in cancer patients. Hepatogastroenterology 1997; 44(17): 1519–1526.
42. Nara-Ashizawa N, Akiyama Y, Maruyama K, Tsukada T, Yamaguchi K. Lipolytic and lipoprotein lipase (LPL)-inhibiting activities produced by a human lung cancer cell line responsible for cachexia induction. Anticancer Res 2001;21(5):3381–3387.
43. Hozumi Y, Kawano M, Hakamata Y, Miyata M, Jordan VC. Tamoxifen inhibits lipoprotein activity: In vivo and in vitro studies. Horm Res 2000;53(1):36–39.
44. Onken MD, Ehlers JP, Worley LA, Makita J, Yokota Y, Harbour JW. Functional gene expression analysis uncovers phenotypic switch in aggressive uveal melanomas. Cancer Res 2006;66(9): 4602–4609.

International Journal of Urology (2008) 15, 520–523 doi: 10.1111/j.1442-2042.2008.02042.x

Original Article: Clinical Investigation

Prediction of extraprostatic extension by prostate specific antigen velocity, endorectal MRI, and biopsy Gleason score in clinically localized prostate cancer

Koshiro Nishimoto,[1] Jun Nakashima,[1] Akinori Hashiguchi,[2] Eiji Kikuchi,[1] Akira Miyajima,[1] Ken Nakagawa,[1] Takashi Ohigashi,[1] Mototsugu Oya[1] and Masaru Murai[1]

Departments of [1]Urology and [2]Pathology, Keio University School of Medicine, Tokyo, Japan

Objectives: To investigate the clinical value of prostate specific antigen velocity (PSAV) in predicting the extraprostatic extension of clinically localized prostate cancer.

Methods: One hundred and three patients who underwent radical prostatectomy for clinically localized prostate cancer were included in the analysis. The correlation between preoperative parameters, including PSA-based parameters, clinical stage, and histological biopsy findings, and the pathological findings were analyzed. Logistic regression analysis was performed to identify a significant set of independent predictors for the local extent of the disease.

Results: Sixty-four (60.2%) patients had organ confined prostate cancer and 39 (39.8%) patients had extraprostatic cancer. The biopsy Gleason score, PSA, PSA density, PSA density of the transition zone, and PSAV were significantly higher in the patients with extraprostatic cancer than in those with organ confined cancer. Multivariate logistic regression analysis indicated that the biopsy Gleason score, endorectal magnetic resonance imaging findings, and PSAV were significant predictors of extraprostatic cancer ($P < 0.01$). Probability curves for extraprostatic cancer were generated using these three preoperative parameters.

Conclusions: The combination of PSAV, endorectal magnetic resonance imaging findings, and biopsy Gleason score can provide additional information for selecting appropriate candidates for radical prostatectomy.

Key words: extraprostatic extension, Gleason score, prediction, PSA velocity, radical prostatectomy.

Introduction

Radical prostatectomy is most effective when the disease is organ confined at the time of surgery.[1] However, a significant number of patients undergoing radical prostatectomy for clinically localized prostate cancer are found to have extraprostatic extension in the final pathological analysis.[2–4] Extraprostatic extension of prostate cancer in pathological specimens has been clearly shown to be an unfavorable prognostic finding in patients undergoing radical prostatectomy.[1] Thus, an accurate preoperative assessment of disease extent is essential for the selection of appropriate therapy in patients with prostate cancer. Unfortunately, current clinical methods used preoperatively to predict the disease extent are still of limited value.

Many investigators have tried to combine various preoperative features, such as PSA, biopsy Gleason score, and clinical stage to predict the final pathological stage of radical prostatectomy specimens.[5] Partin *et al.* have reported that the combination of clinical stage from digital rectal examination (DRE), PSA, and Gleason score predicted the pathological stage more accurately than any indicator alone (Partin Tables).[2–4] However, it is generally agreed that DRE is limited by a significant level of clinical understaging, and that the incidence of unsuspected periprostatic soft tissue invasion after prostatectomy in DRE-based staging series is high.[6] Therefore, using other more accurate imaging studies might provide additional information to that reported by Partin *et al.*

PSA is a valuable tumor marker for detecting, staging, and monitoring prostate cancer.[7] In addition to cancer detection, various PSA-based parameters have been shown to be valuable to some extent for the prediction of extraprostatic disease in radical prostatectomy.[8–17] Combinations of PSA-based parameters and other staging methods are required for accurate prediction of the pathological stage. However, the predictive values of the combinations of the PSA-based parameters and other staging modalities have yet to be determined. It has been previously reported that the combination of PSA density (PSAD), endorectal MRI findings, and biopsy Gleason score can provide useful information concerning the pathological stage.[18] In that study, PSAD was the most valuable predictor among the PSA-based parameters for detecting extraprostatic disease in patients with clinically localized prostate cancer. However PSA velocity (PSAV) was not included in the previous study in spite of PSAV having been widely watched after the report to be a strong and independent predictor of tumor stage,[19] biochemical progression and death from prostate cancer.[20] The present study was undertaken to investigate the clinical value of PSAV, in comparison with other parameters including PSA and PSAD, for the prediction of extraprostatic disease.

Methods

The present study consisted of 103 patients (mean age, 66.4 ± 5.3 years, range 51–74 years) who underwent radical prostatectomy and pelvic lymphadenectomy for clinically localized prostate cancer at our institution. The mean length of PSA follow up before surgery was 27.9 ± 24.1 (range, 6.3–106.2) months. Patients who had received endocrine therapy prior to radical prostatectomy and for whom there were no PSAV data were excluded. Prostate cancer was histologically confirmed preoperatively by transrectal ultrasound-guided needle biopsy using a 10-MHz endorectal transducer. The staging procedures included DRE, computed tomography, endorectal magnetic resonance

Correspondence: Jun Nakashima MD, Department of Urology, Keio University School of Medicine, 35 Shinanomachi, Shinjuku, Tokyo, Japan. Email: njun@sc.itc.keio.ac.jp

Received 11 October 2007; accepted 13 February 2008.
Online publication 15 April 2008

Table 1 Comparison of preoperative parameters in patients with organ confined prostate cancer and those with extraprostatic cancer

	Organ confined (mean ± SE)	Extraprostatic (mean ± SE)	*P*-value
No. of patients	64	39	
Gleason score	5.719 ± 0.129	6.231 ± 0.206	0.0285
P volume (cc)	39.317 ± 2.070	31.973 ± 1.859	0.017
TZ volume (cc)	19.579 ± 1.560	13.551 ± 1.166	0.0072
PSA (ng/ml)	8.375 ± 0.448	11.758 ± 1.284	0.0041
PSAD	0.239 ± 0.016	0.415 ± 0.051	0.0001
PSATZD	0.603 ± 0.070	1.105 ± 0.144	0.0007
PSAV (ng/mL/year)	0.962 ± 0.213	3.197 ± 0.655	0.0002

PSA, prostate specific antigen; PSAD, PSA density; PSATZD, PSA density of the transition zone; PSAV, PSA velocity; TZ, transition zone.

imaging (MRI), and bone scanning. All endorectal MRI studies were performed more than 4 weeks after prostate biopsy to reduce the possibility of postbiopsy artifacts. Tumors which attached to the prostate capsule more than 1 cm in width on endorectal MRI and tumors with a localized bulge were defined as a subgroup of suspected microscopic extension, while tumors with a contact length of less than 1 cm were defined as a subgroup of no extension.[18,21] Patients who had definite findings of extracapsular extension and/or seminal vesicle involvement on endorectal MRI were excluded from this study. The prostate volume was calculated based on a prolate ellipsoid and the length was measured using transrectal ultrasound. Serum samples were obtained before DRE. PSA concentrations were determined by an enzyme immunoassay (AIA-PACK PA; Tosoh Company, Foster City, CA). PSAD and the PSA density of the transition zone (PSATZD) were calculated by dividing the PSA value by prostate volume and transition zone volume (TZ volume). The surgical specimens were step sectioned at 4 mm intervals perpendicular to the long axis of the gland and each section examined. Whole mount preparations were used to assess extraprostatic cancer. Extraprostatic cancer was defined as seminal vesicle involvement, malignant cells outside the prostatic capsule, or lymph node metastasis. The three consecutive PSA data were recorded as the value at first visit to our office as PSA1, the closest value in time before diagnosis as PSA3, and the value at the mid-point in time between PSA1 and PSA3 as PSA2. Using these three consecutive PSA values, PSAV were calculated as shown below using the method that was previously reported by Carter and Pearson.[22] All PSA data were measured at our institution.

$$X1 = (PSA2 - PSA1)/\text{period from PSA1 to PSA2}$$
$$X2 = (PSA3 - PSA2)/\text{period from PSA2 to PSA3}$$
$$\text{PSA velocity} = (X1 + X2)/2$$

The groups were compared using the Mann–Whitney *U*-test. The independence of fit of categorized data was analyzed with the χ^2 test. Receiver operating characteristic (ROC) curves were plotted with the sensitivity (true-positive fraction) on the *y*-axis versus 1 minus the specificity (false-positive fraction) on the *x*-axis. Independent factors for the prediction of extraprostatic cancer were identified using stepwise logistic regression analysis. The predicted probability of extraprostatic cancer was estimated as $P = 1/(1 + \exp^{-k})$. Logistic regression gives a score (k), where k is $a + b1 \times 1 + b2 \times 2 + \ldots$, which is a linear combination of the predictors ($\times 1$, $\times 2$ ...) in the model. The model coefficients (a, b1, b2 ...) were chosen to optimize the model's ability to predict the probability of extraprostatic cancer. Differences were considered statistically significant at $P < 0.05$.

Results

A total of 64 (60.2%) patients had organ confined cancer in the pathological specimen while 39 (39.8%) patients had extraprostatic cancer including 37 (94.9%) patients with only extracapsular extension, 2 (5.1%) with seminal vesicle invasion, and no lymph node metastasis. Preoperative parameters in both groups are summarized in Table 1. Significant differences were noted in prostate volume ($P = 0.0170$), TZ volume ($P = 0.0072$), Gleason score ($P = 0.0285$) in the biopsy specimens, preoperative PSA ($P = 0.0041$), PSAD ($P = 0.0001$), PSATZD ($P = 0.0007$), and PSAV ($P = 0.0002$) between patients with organ confined cancer and those with extraprostatic cancer.

Based on DRE findings, 82 (79.6%) patients were classified as stage T1c and 21 (20.4%) were classified as either stage T2a or T2b. Fifty-two patients with a T1c tumor (63.4%) and 12 patients with T2a or T2b tumor (57.1%) had pathologically organ confined cancer. No significant correlation was found between the DRE findings and the pathological findings.

On the other hands, endorectal MRI demonstrated no extension in 84 patients, while it demonstrated suspected microscopic extension in 19. Among the no extension on endorectal MRI subgroup, 71.4% (60/84) had pathologically organ confined cancer, while 78.9% (15/19) of the suspected microscopic extension subgroup had pathologically extraprostatic cancer. A significant correlation was found between the endorectal MRI findings and the pathological findings ($P = 0.0001$).

The area under the ROC curve (AUC) was calculated in order to estimate the predictive value of the preoperative parameters for the prediction of extraprostatic cancer. The AUC was 0.612 for PSA, 0.626 for prostate volume, 0.647 for TZ volume, 0.612 for PSA, 0.685 for PSAD, 0.702 for PSATZD, and 0.706 for PSAV. The *P*-value between PSAV and PSA, between PSAV and PSAD and between PSAV and PSATZD were 0.44, 0.86, and 0.97, respectively, which were not significant. Although the *P*-values were not significant among these AUC, PSAV had the largest AUC value among the PSA-based parameters.

Multivariate stepwise logistic regression analysis was performed to assess the significant independent preoperative parameters to predict extraprostatic cancer. The analysis indicated that biopsy Gleason score (≤6 *vs* 7≤), endorectal MRI findings (no extension *vs* suspected

Table 2 Multivariate stepwise logistic regression analysis to predict extraprostatic prostate cancer

	P-value	Odds ratio	95% CI
Gleason score (≤6 *vs* ≥7)	0.0009	5.823	1.971–17.200
MRI findings	0.0002	10.501	2.694–40.938
PSAV	<0.0001	1.399	1.143–1.712

MRI, magnetic resonance imaging; PSAV, prostate specific antigen velocity.

microscopic extension), and PSAV were significant predictors of the extraprostatic extension of prostate cancer ($P = 0.0009$, 0.0002, and <0.0001, respectively, Table 2).

Probability curves for extraprostatic cancer were generated using the three preoperative parameters (PSAV, endorectal MRI findings, and biopsy Gleason score). Figure 1 shows plots representing the probability of extraprostatic cancer by a combination of the preoperative parameters. For example, a patient with a PSAV of 2 ng/mL/year, no extraprostatic extension on endorectal MRI, and a biopsy Gleason score 7≤ has a 57.5% probability of pathological extraprostatic cancer (Fig. 1).

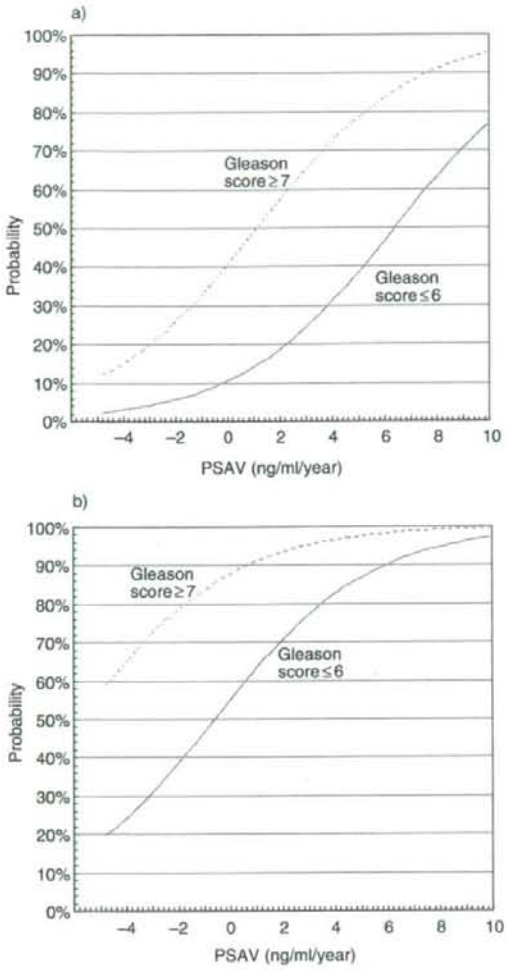

Fig. 1 Probability plots for predicting extraprostatic prostate cancer by biopsy Gleason score, prostate specific antigen velocity, and endorectal magnetic resonance imaging findings. (a) No extension on endorectal MRI. (b) Microscopic extension suspected on endorectal MRI.

Discussion

Although staging evaluation of prostate cancer with various preoperative examinations may increase the percentage of cases being correctly diagnosed as organ confined cancer, preoperative staging tends to understage a significant number of patients, which often results in additional treatment. Therefore, accurate prediction of the local extent of prostate cancer by means of preoperative variables is crucial with respect to making a decision concerning treatment strategy. Identification of the preoperative parameters predictive of the pathological stage at radical prostatectomy has become a topic of major concern. In the present study, patients with clinically localized prostate cancer who were preoperatively evaluated by endorectal MRI and had undergone radical prostatectomy were studied to determine the preoperative variables that were significantly associated with extraprostatic extension. The results demonstrated that preoperative PSAV, biopsy Gleason score, and endorectal MRI findings are the best combination of predictors for the extraprostatic extension of prostate cancer. Partin *et al.* contributed greatly to the clinical assessment of prostate cancer through their nomograms for predicting the pathological stage using preoperative PSA, biopsy Gleason score, and clinical stage using DRE.[2-4] Various nomograms are currently available for predicting the final pathological stage and biochemical recurrence free survival based on preoperative parameters.[5] Although these nomograms appear to be cost effective and good predictors of the final pathological stage, there is still room for improvement. The introduction of endorectal MRI has improved the ability to correctly define local tumor staging. However, it seems to have limitations with respect to the diagnosis of microscopic extraprostatic cancer.[23,24] To overcome the limitations of endorectal MRI, other staging modalities, including PSA-based parameters and biopsy findings, should be combined with endorectal MRI staging. Although PSA is widely used for the early detection, staging, and monitoring of patients with prostate cancer, the use of PSA alone as a tumor marker is not sufficiently sensitive or specific for staging.[3-4,7] In recent years, several PSA-based parameters, such as percent free PSA, PSAD, PSATZD, and PSA-ACT have been evaluated and compared to clarify whether they could be used as superior preoperative predictors of extracapsular tumor invasion.[8-18] In a previous study, multivariate logistic regression analysis demonstrated that PSAD was a significant predictor of the postoperative pathological outcome among these PSA-based parameters, as were endorectal MRI findings and the biopsy Gleason score.[18] However, PSAV was not included as one of the PSA-based parameters.

In the present study, we investigated the clinical value of PSAV with PSAD. Previous studies have reported that the rate of change of PSA, such as PSAV and PSA doubling time before the diagnosis of prostate cancer, can predict tumor stage, grade, and the time to recurrence after

radical prostatectomy.[19,22,25] Moreover, D'Amico *et al.*[20] have recently reported that men whose PSA level increases by more than 2.0 ng per milliliter during the year before the diagnosis of prostate cancer may have a relatively high risk of death from prostate cancer despite undergoing radical prostatectomy. In the present study, PSA, PSAD, PSATZD, and PSAV were significantly higher in patients with extraprostatic cancer than in those with organ confined disease. In addition, the area under the ROC curve for PSAV was slightly larger than that for PSAD or PSATZD. Furthermore, multivariate stepwise logistic regression analysis demonstrated that PSAV was the best predictor of extraprostatic disease among these possible PSA-based parameters. Therefore, PSAV is considered to be equal or superior to PSAD or PSATZD for predicting the local extent of the disease. Although PSAV is not always available for all patients, the clinical value of PSAV is thought to be significant in patients who have had their PSA determined more than two times. In addition, since PSAV was retrospectively calculated, there is a limitation that the intervals of the PSA measurements are not uniform among respective PSAV calculation in this study.

In conclusion, the present study has demonstrated that preoperative PSAV, like endorectal MRI findings and biopsy Gleason score, can be a good predictor of extraprostatic disease in patients with clinically localized prostate cancer. Although it is anticipated that our result for predicting extraprostatic cancer will be validated by other investigators in the future, the combination of PSAV, endorectal MRI findings, and biopsy Gleason score may provide additional information that will assist in selecting appropriate candidates for radical prostatectomy.

References

1 Hull GW, Rabbani F, Abbas F, Wheeler TM, Kattan MW, Scardino PT. Cancer control with radical prostatectomy alone in 1000 consecutive patients. *J. Urol.* 2002; **167**: 528–34.

2 Partin AW, Kattan MW, Subong EN *et al.* Combination of prostate-specific antigen, clinical stage, and Gleason score to predict pathological stage of localized prostate cancer. A multi-institutional update. *JAMA* 1997; **277**: 1445–51.

3 Partin AW, Mangold LA, Lamm DM, Walsh PC, Epstein JI, Pearson JD. Contemporary update of prostate cancer staging nomograms (Partin Tables) for the new millennium. *Urology* 2001; **58**: 843–8.

4 Partin AW, Yoo J, Carter HB *et al.* The use of prostate specific antigen, clinical stage and Gleason score to predict pathological stage in men with localized prostate cancer. *J. Urol.* 1993; **150**: 110–14.

5 Ross PL, Scardino PT, Kattan MW. A catalog of prostate cancer nomograms. *J. Urol.* 2001; **165**: 1562–8.

6 Perrotti M, Pantuck A, Rabbani F, Israeli RS, Weiss RE. Review of staging modalities in clinically localized prostate cancer. *Urology* 1999; **54**: 208–14.

7 Polascik TJ, Oesterling JE, Partin AW. Prostate specific antigen: a decade of discovery – what we have learned and where we are going. *J. Urol.* 1999; **162**: 293–306.

8 Furuya Y, Ohta S, Sato N *et al.* Prostate-specific antigen density adjusted for the transition zone for staging clinically localized prostate cancer in Japanese patients with intermediate serum prostate-specific antigen levels. *Anticancer Res.* 2001; **21**: 1317–20.

9 Graefen M, Karakiewicz PI, Cagiannos I *et al.* Percent free prostate specific antigen is not an independent predictor of organ confinement or prostate specific antigen recurrence in unscreened patients with localized prostate cancer treated with radical prostatectomy. *J. Urol.* 2002; **167**: 1306–9.

10 Hara I, Miyake H, Hara S *et al.* Value of the serum prostate-specific antigen-alpha 1-antichymotrypsin complex and its density as a predictor for the extent of prostate cancer. *BJU Int.* 2001; **88**: 53–7.

11 Kurita Y, Suzuki A, Masuda H, Ushiyama T, Suzuki K, Fujita K. Transition zone volume -adjusted prostate-specific antigen value predicts extracapsular carcinoma of the prostate in patients with intermediate prostate-specific antigen levels. *Eur. Urol.* 1998; **33**: 32–8.

12 Melchior SW, Noteboom J, Gillitzer R, Lange PH, Blumenstein BA, Vessella RL. The percentage of free prostate-specific antigen does not predict extracapsular disease in patients with clinically localized prostate cancer before radical prostatectomy. *BJU Int.* 2001; **88**: 221–5.

13 Morote J, Encabo G, de Torres IM. Use of percent free prostate-specific antigen as a predictor of the pathological features of clinically localized prostate cancer. *Eur. Urol.* 2000; **38**: 225–9.

14 Pannek J, Rittenhouse HG, Chan DW, Epstein JI, Walsh PC, Partin AW. The use of percent free prostate specific antigen for staging clinically localized prostate cancer. *J. Urol.* 1998; **159**: 1238–42.

15 Thiel R, Pearson JD, Epstein JI, Walsh PC, Carter HB. Role of prostate-specific antigen velocity in prediction of final pathologic stage in men with localized prostate cancer. *Urology* 1997; **49**: 716–20.

16 Tombal B, Querton M, de Nayer P *et al.* Free/total PSA ratio does not improve prediction of pathologic stage and biochemical recurrence after radical prostatectomy. *Urology* 2002; **59**: 256–60.

17 Zlotta AR, Djavan B, Petein M, Susani M, Marberger M, Schulman CC. Prostate specific antigen density of the transition zone for predicting pathological stage of localized prostate cancer in patients with serum prostate specific antigen less than 10 ng/mL. *J. Urol.* 1998; **160**: 2089–95.

18 Horiguchi A, Nakashima J, Horiguchi Y *et al.* Prediction of extraprostatic cancer by prostate specific antigen density, endorectal MRI, and biopsy Gleason score in clinically localized prostate cancer. *Prostate* 2003; **56**: 23–9.

19 Egawa S, Arai Y, Tobisu K *et al.* Use of pretreatment prostate-specific antigen doubling time to predict outcome after radical prostatectomy. *Prostate Cancer Prostatic Dis.* 2000; **3**: 269–74.

20 D'Amico AV, Chen MH, Roehl KA, Catalona WJ. Preoperative PSA velocity and the risk of death from prostate cancer after radical prostatectomy. *N. Engl. J. Med.* 2004; **351**: 125–35.

21 Nakashima J, Tanimoto A, Imai Y *et al.* Endorectal MRI for prediction of tumor site, tumor size, and local extension of prostate cancer. *Urology* 2004; **64**: 101–5.

22 Carter HB, Pearson JD. PSA velocity for the diagnosis of early prostate cancer. A new concept. *Urol. Clin. North Am.* 1993; **20**: 665–70.

23 Cornud F, Flam T, Chauveinc L *et al.* Extraprostatic spread of clinically localized prostate cancer: factors predictive of pT3 tumor and of positive endorectal MR imaging examination results. *Radiology* 2002; **224**: 203–10.

24 Ikonen S, Karkkainen P, Kivisaari L *et al.* Magnetic resonance imaging of prostatic cancer: does detection vary between high and low Gleason score tumors? *Prostate* 2000; **43**: 43–8.

25 Goluboff ET, Heitjan DF, DeVries GM, Katz AE, Benson MC, Olsson CA. Pretreatment prostate specific antigen doubling times: use in patients before radical prostatectomy. *J. Urol.* 1997; **158**: 1876–8; discussion 8–9.

BJUI BJU INTERNATIONAL

Prostate-specific antigen 'bounce' after permanent ^{125}I-implant brachytherapy in Japanese men: a multi-institutional pooled analysis

Takefumi Satoh*, Hiromichi Ishiyama†, Kazumasa Matsumoto*, Hideyasu Tsumura*, Masashi Kitano†, Kazushige Hayakawa†, Shin Ebara†, Yasutomo Nasu†, Hiromi Kumon†, Susumu Kanazawa‡, Kenta Miki¶, Shin Egawa¶, Manabu Aoki, Kazuhito Toya††, Atsushi Yorozu††, Hirohiko Nagata††, Shiro Saito†† and Shiro Baba***

*Departments of *Urology and †Radiology, Kitasato University School of Medicine, Kanagawa, Departments of †Urology and ‡Radiology, Okayama University Graduate School of Medicine, Okayama, Departments of ¶Urology and **Radiology, Tokyo University School of Medicine, Jikei, and Departments of ††Radiology and ††Urology, National Hospital Organization Tokyo Medical Center, Tokyo, Japan*

Accepted for publication 21 August 2008

Study Type – Prognosis (case series)
Level of Evidence 4

OBJECTIVE

To examine the incidence, timing, and magnitude of the prostate-specific antigen (PSA) level 'bounce' after permanent prostate brachytherapy (BT) and correlate the PSA bounce with clinical and dosimetric factors in Japanese patients with prostate cancer.

PATIENTS AND METHODS

A multi-institutional pooled analysis was carried out in 388 consecutive patients with T1–T2N0M0 prostate cancer treated with ^{125}I-seed implant BT with no hormonal therapy or external beam radiotherapy. All patients had ≥1 year of follow-up and at least three follow-up PSA level measurements. Three definitions of PSA bounce were used: definition A, a PSA level rise of 0.1 ng/mL; definition B, a PSA level rise of 0.4 ng/mL; and definition C, a PSA level rise of 35% over the previous value, followed by a subsequent fall.

RESULTS

The actuarial likelihood of having PSA bounce at 24 months was 50.8% for definition A, 23.5% for definition B, and 19.4% for definition C. The median time to develop PSA bounce was 12 months for definition A, 18 months for definition B, and 18 months for definition C. There was a PSA bounce magnitude of 2 ng/mL in 5.3% of patients, and 95.3% of PSA bounce occurred within 24 months after ^{125}I-BT. Among the before and after ^{125}I-BT factors, clinical stage, initial PSA level, and Gleason score did not predict for PSA bounce using any definition; only being younger predicted for PSA bounce on multivariate analysis ($P < 0.001$).

CONCLUSIONS

PSA bounce is a common phenomenon after ^{125}I-BT and occurred at a rate of 19–51% in the Japanese men who underwent ^{125}I-BT, depending on the definition used. It is more common in younger patients, and early PSA bounce should be considered when assessing a patient with a rising PSA level after ^{125}I-BT, before implementing salvage interventions. Furthermore, PSA bounce magnitude might be lower in Japanese than in Caucasian patients.

KEYWORDS

prostate cancer, prostate-specific antigen (PSA) bounce, brachytherapy

INTRODUCTION

Prostate permanent brachytherapy (BT) is currently available and becoming a commonly used method for treating prostate cancer in Japan. One of the most appealing reasons for selecting this treatment is the low degree of toxicity, which may reduce the impact on quality of life in the patient [1,2]. However, PSA kinetics after this treatment is different from that after radical prostatectomy. It is generally thought that the PSA level continuously decreases after potentially successful radiation for prostate cancer and that an increase in PSA levels might reflect disease recurrence. However, physicians often observe a temporary increase in PSA levels after radiation therapy for prostate cancer, which does not reflect disease recurrence. This phenomenon is called PSA 'bounce' (spikes), and 30–50% of patients treated with BT have PSA bounce [3,4].

The PSA bounce is thought to be the result of compromised membrane integrity in the PSA-producing epithelium and has not proved to be of prognostic consequence in patients treated with BT [5]. However, still unclear, are not only the mechanism of PSA bounce, but also ethnic/racial differences of PSA bounce after BT.

 | doi:10.1111/j.1464-410X.2008.08234.x

The present study is the first to examine PSA bounce after BT alone, with no hormonal therapy or external beam radiotherapy (EBRT), in Japanese men with prostate cancer. In addition, the effect of pretreatment and treatment-related factors on PSA bounce were analysed to determine which patients were at increased risk of developing PSA bounce.

PATIENTS AND METHODS

In all, 388 patients underwent an ^{125}I-permanent implant. No patient received hormonal therapy or EBRT. Eligible patients for the study had to have ≥1 year of follow-up and at least three PSA measurements after treatment. The PSA level was measured at 1 month after implant and at 3-month follow-up intervals within 2 years after implant, and 6-month follow-up intervals thereafter.

The prescribed dose to the periphery of the prostate was 145 Gy using a prostate implant technique that has been previously described [1,6]. Both before and after implant analyses used a radiotherapy planning system dedicated for transperineal interstitial permanent prostate BT (Interplant version 3.4 CMS or Variseed version 7.1 VARIAN), and all doses were defined using TG43 criteria [7]. At 1 month after implant, a CT-based dosimetric analysis was performed. Dosimetry data were available for all patients after implant. To analyse the effect of dose on PSA bounce, dose was defined as the dose delivered to 90% of the gland on the 1-month after implant dose-volume histogram (D_{90}).

A PSA bounce was defined as an elevation of the PSA level (at any time an elevation occurred, excluding the 1-month PSA value) from the previous value with a subsequent fall. Three descriptions of a PSA bounce were used: definition A, a rise of 0.1 ng/mL; definition B, a rise of 0.4 ng/mL; and definition C, a rise of >35% over the previous value [4].

Associations between PSA bounce and the before treatment and treatment-related factors were examined using logistic regression analysis.

RESULTS

The patient clinical disease characteristics and dosimetric variables are shown in Table 1. The median percentage of the prostate volume receiving a minimum of 100% of the prescribed dose (V_{100}) was 94.7%, and the median minimum D_{90} was 158.9 Gy. The median (range) follow-up for the entire group was 30 (12–42) months. The actuarial likelihood of having PSA bounce at 24 months was 50.8% for definition A, 23.5% for definition B, and 19.4% for definition C (Fig. 1).

Variable	Value
Median (range):	
Age, years	67 (47–83)
Initial PSA level, ng/mL	6.6 (0.6–23.5)
N:	
Clinical stage	
T1	324
T2	64
Gleason score	
≤6	272
7	106
≥8	10
Median (range):	
Prostate volume, cm^3	26.2 (5.0–51.1)
PSAD, ng/mL/cm^3	0.28 (0.05–1.16)
V_{100}, %	94.7 (60.2–100)
V_{150}, %	63.0 (21.5–98.4)
D_{90}, Gy	158.9 (69–239.5)

TABLE 1
The patients' characteristics before treatment and dosimetric variables after treatment

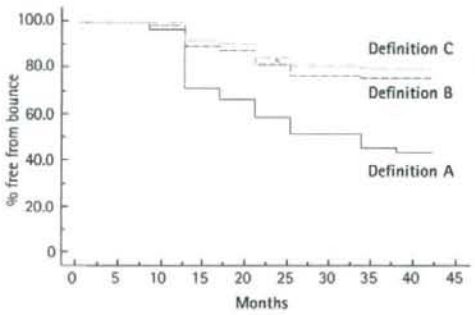

FIG. 1.
Actuarial analyses of PSA bounce for the three definitions.

The distribution of the time of onset of PSA bounce is shown in Fig. 2A, based on definition A. The median time to PSA bounce was 12 months for definition A, 18 months for definition B, and 18 months for definition C; 95.3% (164/172) of PSA bounce was seen within 24 months after ^{125}I-BT for definition A.

The median (range) before bounce PSA level was 1.09 (0.11–5.74) ng/mL, and the median (range) bounce height (increase above the before bounce level) was 0.40 (0.1–6.62) ng/mL. The magnitudes of the bounce were 0.1–0.2 ng/mL in 26.7%, 0.2–0.4 ng/mL in 22.1%, 0.4–1.0 ng/mL in 35.4%, 1.0–2.0 ng/mL in 10.5%, 2.0–5.0 ng/mL in 4.1%, and >5 ng/mL in 1.2% (Fig. 2B).

The effects of patient age, initial PSA level, Gleason score, clinical stage, prostate volume, PSA density, D_{90}, V_{100}, and the prostate volume receiving at least 150% dose at 1 month (V_{150}) on developing a PSA bounce were tested using univariate analysis with each of the three definitions (Table 2). Using definition A, age, prostate volume, and PSA density (PSAD) significantly affected the incidence of bounce ($P < 0.001$, $P = 0.018$, $P = 0.009$, respectively). Using definition B, patient age and prostate volume significantly affected the incidence of bounce ($P < 0.001$, $P = 0.041$, respectively). Using definition C, patient age also significantly affected the incidence of bounce ($P = 0.001$). The multivariate Cox regression

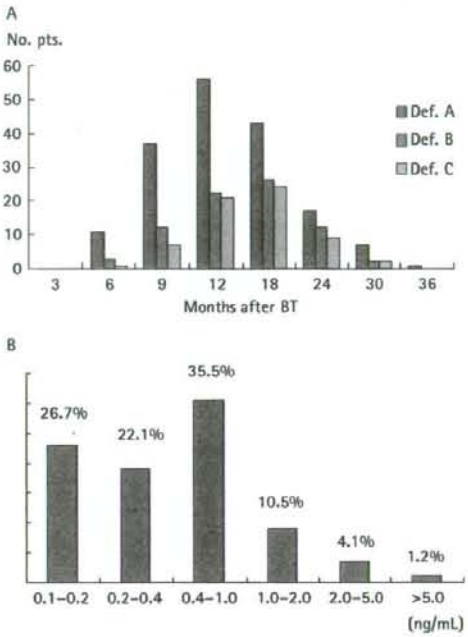

FIG. 2.
A, Histogram of the time to develop PSA bounce (in months) after prostate BT. Bars show the rise for each of the definitions (definition A, a rise of 0.1 ng/mL; definition B, a rise of 0.4 ng/mL; and definition C, a rise of >35% over the previous value). B, Distribution of magnitude of PSA bounce.

analysis determined predictors for PSA bounces are listed in Table 3. On multivariate analysis, only patient age predicted a PSA bounce ($P < 0.001$) using definition A. Using definition B, patient age and prostate volume predicted PSA bounce on multivariate analysis ($P < 0.001$, $P = 0.029$, respectively).

DISCUSSION

It is well known that PSA is a kallikrein III, seminin, semenogelase, â-seminoprotein, and P-30 antigen and is a 34-kDa glycoprotein manufactured by the cells of the prostate gland. PSA is present in small quantities in the serum of normal men and is often elevated in the presence of prostate cancer and other prostate disorders. The Hybritech Tandem-R PSA test, released in 1986 [8], is a blood test to measure PSA concentration and is widely used not only for detection of prostate cancer, but also as a follow-up tool after treatment.

It is also well known that PSA level changes after prostate BT show a gradual decline, unlike radical prostatectomy. The PSA values may take >5 years to reach a nadir [9]. The intact prostate, with its normal and abnormal epithelial cells, is the source for these PSA fluctuations. A PSA bounce after prostate BT causes anxiety not only in patients, but also in physicians.

PSA bounce after permanent seed BT has been reported by several investigators, and it is common, occurring in 20–40% of men after prostate BT. Various definitions have been reported, and Critz *et al.* [3] originally reported the phenomenon based on 779 men treated with simultaneous radiotherapy with a ^{125}I-prostate implant followed by EBRT. They defined PSA bounce as an increase of ≥0.1 ng/mL above the preceding PSA level after simultaneous radiation followed by a subsequent decrease below that level. PSA bounce occurred in 35% of the men, and the median time to PSA bounce was 18 months from the time of implant, with 92% of bounce occurring within 36 months. Stock *et al.* [4] reported that PSA bounce is more common in patients with higher implant doses and in younger patients. The patients receiving an implant dose of ≤160 Gy had a PSA bounce rate at 5 years of 24% vs 38% for those receiving an implant dose of >160 Gy, and younger patients (aged ≤65 years) had a PSA bounce rate at 5 years of 38% vs. 24% for older patients. Crook *et al.* [10] reported that PSA bounce occurred in 40% of men and that the only clinical or dosimetric factor predictive of PSA bounce in multivariate analysis was being younger. Bostancic *et al.* [5] reported that the incidence of PSA bounce was substantially different in patients aged <65 years vs ≥65 years (38.5% vs 16.3%), and patient age and isotope were significant predictors for PSA bounce.

There is little agreement on risk factors associated with PSA bounce; however, several articles have reported that age is a predictor for PSA bounce after BT. In the present study, there was a significant correlation between age and PSA bounce in a Japanese setting, and it is a common phenomenon not only among Caucasians, but also Japanese. Crook *et al.* [10] reported that the median magnitude of PSA bounce was 0.76 ng/mL and that 64% had a magnitude of <1 ng/mL, 21% had a magnitude of 1–2 ng/mL, and 15% had a magnitude >2 ng/mL, surprisingly. In the present study, the median magnitude of the PSA bounce was 0.40 ng/mL and 84.3% had a magnitude <1 ng/mL, 10.5% had a magnitude of 1–2 ng/mL, and 5.3% had a magnitude >2 ng/mL.

Compared to our current study, frequency and onset of PSA bounce were closed to our results. However, PSA bounce height in Japanese patients was lower than in Caucasian patients. The reason for this difference is not clear; however, PSA bounce height may also be related to the duration of follow-up. Therefore, this should be considered in the present study where the follow-up was of limited duration.

The underlying mechanism of PSA bounce and the reasons for the influence of age on this bounce are still unknown. The first potential hypothesis is that PSA bounce might be due to a late-developing radiation reaction such as radiation prostatitis. Cesaretti *et al.* [11] reported on a late complication of ^{125}I-BT, which they have termed urinary symptom flare. The time to develop a 'flare' ranged from 5.8 to 64 months (median 23.9 months). A transient late exacerbation of urinary symptoms is common and can occur in up to half of all patients by 5 years after ^{125}I-BT. Lehers *et al.* [12] also reported that after BT for prostate cancer, some patients had recurrent LUTS after an asymptomatic period; this secondary exacerbation of symptoms ('symptom flare') occurred at ≈2 years after implantation, and this time-frame might correspond to PSA bounce.

TABLE 2 Univariate analysis of factors potentially affecting PSA bounce

Variable	Bounce	Definition A Median (range)	*P*	Definition B Median (range)	*P*	Definition C Median (range)	*P*
Age, years							
	Yes	65 (47–79)	<0.001	63 (47–79)	<0.001	62.5 (47–76)	0.001
	No	68 (52–83)		68 (49–83)		67.5 (49–83)	
Initial PSA, ng/mL							
	Yes	6.4 (0.6–17.8)	0.29	6.9 (1.5–15.6)	0.721	6.8 (1.8–15.6)	0.847
	No	6.7 (2.1–23.5)		6.5 (0.6–23.5)		6.6 (0.6–23.5)	
Gleason score							
	Yes	6 (3–9)	0.349	6 (3–9)	0.534	6 (3–9)	0.831
	No	6 (3–8)		6 (3–9)		6 (3–9)	
Prostate volume, cm^3							
	Yes	27 (7.3–51.1)	0.018	27.2 (7.3–51.1)	0.041	25 (14.9–41.8)	0.769
	No	25.8 (5–50)		25.9 (5–50.6)		26.2 (5–51.1)	
PSAD, $ng/mL/cm^3$							
	Yes	0.25 (0.05–1.0)	0.009	0.26 (0.05–1.0)	0.273	0.29 (0.10–0.82)	0.724
	No	0.29 (0.08–1.16)		0.28 (0.08–1.16)		0.28 (0.05–1.16)	
D_{90}, Gy							
	Yes	156.6 (87.9–227.1)	0.128	159.5 (94.8–227.1)	0.993	157.5 (94.8–227.1)	0.436
	No	160.4 (100.7–239.5)		158.8 (87.9–239.5)		159 (87.9–239.5)	
V_{100}, %							
	Yes	94.3 (73.7–100)	0.344	94.7 (73.7–100)	0.879	94 (75.5–100)	0.817
	No	94.8 (74.3–100)		94.7 (74.3–100)		94.7 (73.7–100)	

TABLE 3 Multivariate analysis of factors potentially affecting PSA bounce

Variable	Definition A Uni.	Multi.	Wald	Exp (B)	Definition B Uni.	Multi.	Wald	Exp (B)	Definition C Uni.	Multi.	Wald	Exp (B)
Age, years	<0.001*	<0.001*	19.837	0.922	<0.001*	<0.001*	20.896	0.906	0.001*	<0.001*	12.597	0.915
Initial PSA level, ng/mL	0.29	–	–	–	0.721	–	–	–	0.847	–	–	–
Gleason score	0.349	–	–	–	0.534	–	–	–	0.831	–	–	–
Prostate volume, cm^3	0.018*	0.075	3.181	1.032	0.041	0.029*	4.739	1.039	0.769	–	–	–
PSAD, $ng/mL/cm^3$	0.009*	0.376	0.784	0.445	0.273	–	–	–	0.724	–	–	–
D_{90}, Gy	0.128	–	–	–	0.993	–	–	–	0.436	–	–	–
V_{100}, %	0.344	–	–	–	0.879	–	–	–	0.817	–	–	–

**Statistically significant; Uni., univariate; Multi., multivariate.*

However, Rosser *et al.* [13] evaluated the effect of patient age on the occurrence of PSA bounce after EBRT for prostate cancer. In all, 12% of the patients developed a PSA bounce, and age was not associated with the occurrence of PSA bounce ($P = 0.63$) after EBRT alone. Therefore, PSA bounce after BT might involve a different mechanism compared with EBRT.

The second hypothesis is that younger patients might have more prostatic epithelium compared with older patients because serum PSA levels correlate significantly with prostatic epithelial volumes [14,15]. The present data suggest that prostate volume might be correlated with PSA bounce, and therefore younger patients are more likely to have inflammation and transient rises. However, the correlation between prostate volume and PSA bounce was weak and only definition B was significant in the multivariate analysis. Further analysis of the mechanism of PSA bounce is needed.

Another hypothesis involves the influence of ejaculation on PSA bounce. Crook *et al.* [10] reported that potency before implantation was significantly predictive of PSA bounce. In addition, Tchetgen *et al.* [16] reported that ejaculation causes a significant increase in the serum PSA concentration in men aged 49–79 years that may persist for up to 48 h. This change appears to correlate with age and baseline PSA levels, and it is recommended that men abstain from ejaculation for 48 h before having a serum PSA determination. However, sexual function correlated with age is usual, and it is still unclear that a correlation exists between the influence of ejaculation and the timing of PSA bounce (the median time to PSA bounce was 18 months).

Finally, we should be aware of the limitations of the present study, because of retrospective data collection and the short follow-up period. In the interim, we think that PSA bounce height might be lower in Japanese patients than in Caucasian patients.

In conclusion, the present study is the first to examine the incidence, timing, and magnitude of the PSA bounce after permanent prostate BT in Japanese patients. PSA bounce is a common phenomenon after ^{125}I-BT in the Japanese population. Physicians should be aware that PSA bounce is more common in younger patients and must be excluded before implementing salvage interventions. Further analysis of the mechanism of PSA bounce is needed.

CONFLICT OF INTEREST

None declared.

REFERENCES

1 **Namiki S, Satoh T, Baba S *et al.*** Quality of life after brachytherapy or radical prostatectomy for localized prostate cancer: a prospective longitudinal study. *Urology* 2006; **68**: 1230–6

2 **Cesaretti JA, Kao J, Stone NN, Stock RG.** Effect of low dose-rate prostate brachytherapy on the sexual health of men with optimal sexual function before treatment: analysis at > or = 7 years of follow-up. *BJU Int* 2007; **100**: 362–7

3 **Critz FA, Williams WH, Benton JB, Levinson AK, Holladay CT, Holladay DA.** Prostate specific antigen bounce after radioactive seed implantation followed by external beam radiation for prostate cancer. *J Urol* 2000; **163**: 1085–9

4 **Stock RG, Stone NN, Cesaretti JA.** Prostate-specific antigen bounce after prostate seed implantation for localized prostate cancer: descriptions and implications. *Int J Radiat Oncol Biol Phys* 2003; **56**: 448–53

5 **Bostancic C, Merrick GS, Butler WM *et al.*** Isotope and patient age predict for PSA spikes after permanent prostate brachytherapy. *Int J Radiat Oncol Biol Phys* 2007; **68**: 1431–7

6 **Ishiyama H, Kitano M, Satoh T *et al.*** Difference in rectal dosimetry between pre-plan and post-implant analysis in transperineal interstitial brachytherapy for prostate cancer. *Radiother Oncol* 2006; **78**: 194–8

7 **Rivard MJ, Coursey BM, DeWerd LA *et al.*** Update of AAPM Task Group, No. 43 Report: a revised AAPM protocol for brachytherapy dose calculations. *Med Phys* 2004; **31**: 633–74

8 **Mytrle JF, Klimley PG, Ivor L *et al.*** Clinical utility of prostate specific antigen (PSA) in the management of prostate cancer. In *Advances in Cancer Diagnostics*. San Diego: Hybritech Inc, 1986: 1–4

9 **Merrick GS, Butler WM, Galbreath RW, Lief JH.** Five-year biochemical outcome following permanent interstitial brachytherapy for clinical T1–T3 prostate cancer. *Int J Radiat Oncol Biol Phys* 2001; **51**: 41–8

10 **Crook J, Gillan C, Yeung I, Austen L, McLean M, Lockwood G.** PSA kinetics and PSA bounce following permanent seed prostate brachytherapy. *Int J Radiat Oncol Biol Phys* 2007; **69**: 426–33

11 **Cesaretti JA, Stone NN, Stock RG.** Urinary symptom flare following I-125 prostate brachytherapy. *Int J Radiat Oncol Biol Phys* 2003; **56**: 1085–92

12 **Lehrer S, Cesaretti J, Stone NN, Stock RG.** Urinary symptom flare after brachytherapy for prostate cancer is associated with erectile dysfunction and more urinary symptoms before implantation. *BJU Int* 2006; **98**: 979–81

13 **Rosser CJ, Kamat AM, Wang X *et al.*** Is patient age a factor in the occurrence of prostate-specific antigen bounce phenomenon after external beam radiotherapy for prostate cancer? *Urology* 2005; **66**: 327–31

14 **Lepor H, Wang B, Shapiro E.** Relationship between prostatic epithelial volume and serum prostate-specific antigen levels. *Urology* 1994; **44**: 199–205

15 **Fukatsu A, Ono Y, Ito M *et al.*** Relationship between serum prostate-specific antigen and calculated epithelial volume. *Urology* 2003; **61**: 370–4

16 **Tchetgen MB, Song JT, Strawderman M, Jacobsen SJ, Oesterling JE.** Ejaculation increases the serum prostate-specific antigen concentration. *Urology* 1996; **47**: 511–6

Correspondence: Takefumi Satoh, Kitasato University School of Medicine – Urology, 1-15-1 Kitasato, Sagamihara, Kanagawa 228-8555, Japan.
e-mail: tsatoh@kitasato-u.ac.jp

Abbreviations: **BT**, brachytherapy; **EBRT**, external beam radiotherapy; **D_{90}**, dose to 90% of the prostate volume at 1 month; **V_{100}**, prostate volume receiving at least 100% dose at 1 month; **V_{150}**, prostate volume receiving at least 150% dose at 1 month; **PSAD**, PSA density.

Research Article

TRIM68 Regulates Ligand-Dependent Transcription of Androgen Receptor in Prostate Cancer Cells

Naoto Miyajima,[1,2] Satoru Maruyama,[1,2] Miyuki Bohgaki,[1] Satoshi Kano,[1] Masahiko Shigemura,[3] Nobuo Shinohara,[2] Katsuya Nonomura,[2] and Shigetsugu Hatakeyama[1]

Departments of [1]Biochemistry and [2]Urology, and [3]First Department of Medicine, Hokkaido University Graduate School of Medicine, Sapporo, Japan

Abstract

The androgen receptor (AR) is a transcription factor belonging to the family of nuclear receptors that mediate the action of androgen. AR plays an important role in normal development of the prostate, as well as in the progression of prostate cancer. AR is regulated by several posttranslational modifications, including phosphorylation, acetylation, and ubiquitination. In this study, we found that the putative E3 ubiquitin ligase TRIM68, which is preferentially expressed in prostate cancer cells, interacts with AR and enhances transcriptional activity of the AR in the presence of dihydrotestosterone. We also found that TRIM68 functionally interacts with TIP60 and p300, which act as coactivators of AR, and synergizes in the transactivation of AR. Overexpression of TRIM68 in prostate cancer cells caused an increase in secretion of prostate-specific antigen (PSA), one of the most reliable diagnostic markers for prostate cancer, whereas knockdown of TRIM68 attenuated the secretion of PSA and inhibited cell growth and colony-forming ability. Moreover, we showed that TRIM68 expression is significantly up-regulated in human prostate cancers compared with the expression in adjacent normal tissues. These results indicate that TRIM68 functions as a cofactor for AR-mediated transcription and is likely to be a novel diagnostic tool and a potentially therapeutic target for prostate cancer. [Cancer Res 2008;68(9):3486–94]

Introduction

Prostate cancer is the most frequently diagnosed malignancy and is the second leading cause of cancer deaths among men in the United States (1). Prostate cancer is a hormonally regulated malignancy, and androgen receptor (AR) plays an important role in disease progression (2). One of the most troubling aspects of prostate cancer progression is the conversion from an androgen-dependent state to an androgen ablation–resistant state, which, at present, defies any effective treatment (3). In majority of end-stage hormone-refractory tumors, AR continues to be expressed and seems to be activated under androgen ablation conditions. Elucidation of the mechanism of AR activation is essential for understanding process of the prostate cancer progression and for identifying possible targets for intervention (4). AR mediates androgen action as a transcriptional factor in collaboration with a number of coregulators. AR up-regulates or down-regulates target gene expressions, depending on coactivators or corepressors (5, 6). Furthermore, activities of AR and coregulators are regulated by posttranslational modifications, such as methylation, phosphorylation, acetylation, and ubiquitination (7–10). However, little is known about the contribution of such processes to AR function.

Ubiquitination is a versatile posttranslational modification mechanism used by eukaryotic cells. The ubiquitin-proteasome pathway involves ubiquitin modification of substrates and sequential degradation by the proteasome (11). Ubiquitin conjugation is catalyzed by ubiquitin-activating enzyme (E1), ubiquitin-conjugating enzyme (E2), and ubiquitin ligase (E3; ref. 12). E3 is a scaffold protein that mediates between the ubiquitin-linked E2 and the substrate. The resulting covalent ubiquitin ligations form polyubiquitinated conjugates that are rapidly detected and degraded by 26S proteasome (13). E3 is thought to be most directly responsible for substrate recognition. E3 ubiquitin ligases thus far identified include members of the homologous to E6-AP carboxyl terminus (HECT), RING finger, and U-box protein families (14–16).

TRIM68 is a member of the tripartite motif-containing protein (TRIM) family defined by the presence of a common domain structure composed of a RING finger, a B-box, and a coiled-coil motif (17). In addition to these motifs, TRIM68 possesses a carboxy-terminal PRY/SPRY domain. TRIM family proteins are involved in a broad range of biological processes, and consistently, their alterations result in diverse pathologic conditions, such as genetic diseases, viral infection, and cancer development (18). It has been reported that TRIM68 is one of the autoantigens associated with Sjögren's syndrome and is a new diagnostic marker for Sjögren's syndrome (19). However, the function of TRIM68 has not been elucidated. Recently, TRIM68 has also been shown to be highly expressed in the prostate compared with its expression in other normal tissues. TRIM21, which is structurally similar to TRIM68 and is also one of the autoantigens associated with Sjögren's syndrome, has been found to bind DNA and has been suggested to act as a transcription factor regulating gene expression (20, 21). TRIM21 has also been shown to be involved in cellular proliferation and cell death (22). Given the highly prostate-specific expression pattern of TRIM68 and the transcriptional function of its related protein, we hypothesized that TRIM68 plays a role in AR-dependent transcription.

In this study, we obtained evidence that TRIM68 is a novel AR-interacting protein and acts as a coactivator of AR, depending on its ubiquitin ligase activity. Furthermore, knockdown of endogenous TRIM68 expression by RNA interference (RNAi) results in suppression of the oncogenic properties of prostate cancer cells. In addition, we found that TRIM68 is significantly up-regulated in human prostate cancers, suggesting that TRIM68 is likely to be a novel diagnostic tool for prostate cancer.

Requests for reprints: Shigetsugu Hatakeyama, Department of Biochemistry, Hokkaido University Graduate School of Medicine, N15, W7, Kita-ku, Sapporo, Hokkaido 060-8638, Japan. Phone: 81-11-706-5899; Fax: 81-11-706-5169; E-mail: hatas@med.hokudai.ac.jp.

doi:10.1158/0008-5472.CAN-07-6059

Materials and Methods

Cell culture. Prostate cancer cell lines LNCaP-FGC, CWR22Rv1, and PC3 were obtained from the American Type Culture Collection. LNCaP and CWR22Rv1 were maintained under an atmosphere of 5% CO_2 at 37°C in RPMI 1640 (Sigma Chemical Co.) supplemented with 10% fetal bovine serum (FBS; Life Technologies Bethesda Research Laboratories). PC3 and HEK293T cell lines were cultured under the same conditions in DMEM (Sigma) with 10% FBS.

Cloning of cDNAs and plasmid construction. Human TRIM68 cDNA was amplified by PCR from HeLa cDNA (Clontech Laboratories, Inc.). The resulting fragment containing the human TRIM68 cDNA was ligated into the pCR3 vector (Invitrogen) with a FLAG tag and into the pFastBacHT vector (Invitrogen). Human AR cDNA was kindly provided by Dr. Sobue (Nagoya University). Deletion mutants of AR cDNA were generated by PCR. Human TIP60 cDNA was kindly provided by Dr. Ikura (Tohoku University).

Recombinant proteins, antibodies, and reagents. His-tagged TRIM68 was expressed in the Sf9 insect cell line using a baculovirus protein expression system (Invitrogen). The recombinant TRIM68 protein was used as immunogen in rabbits. A rabbit polyclonal anti-TRIM68 antibody was generated and then affinity-purified using a recombinant TRIM68-conjugated Sepharose 4B column. Other antibodies used were as follows: mouse monoclonal anti-HA (HA.11/16B12, Covance Research Products), mouse monoclonal anti-FLAG (M5, Sigma), mouse monoclonal anti-ubiquitin (P4D1, Santa Cruz Biotechnology), goat polyclonal anti–prostate-specific antigen (PSA; Santa Cruz), mouse monoclonal anti-AR (Santa Cruz), and mouse monoclonal anti–α-tubulin (Zymed Laboratories). Dihydrotestosterone, dexamethasone, and 17β-estradiol were purchased from Sigma.

Ubiquitination assay. *In vitro* ubiquitination assays were performed as previously described (16). In brief, reaction mixtures containing 4 μg of the recombinant TRIM68 with 0.1 μg recombinant E1 (Boston Biomedica), 1 μg recombinant E2s, 0.5 unit phosphocreatine kinase, 1 μg ubiquitin (Sigma), 25 mmol/L Tris-HCl (pH 7.5), 120 mmol/L NaCl, 2 mmol/L ATP, 1 mmol/L $MgCl_2$, 0.3 mmol/L DTT, and 1 mmol/L creatine phosphate were incubated for 3 h at 30°C. The reaction was terminated by the addition of SDS sample buffer containing 4% β-mercaptoethanol and heating at 95°C for 5 min. Samples were subjected to immunoblotting with anti-ubiquitin and anti-TRIM68 antibodies.

Transfection, immunoprecipitation, and immunoblot analysis. HEK293T cells were transfected by the calcium phosphate method. After 48 h, the cells were lysed in a solution containing 50 mmol/L Tris-HCl (pH 7.4), 150 mmol/L NaCl, 1% Nonidet P-40, leupeptin (10 μg/mL), 1 mmol/L phenylmethylsulfonyl fluoride, 400 μmol/L Na_3VO_4, 400 μmol/L EDTA, 10 mmol/L NaF, and 10 mmol/L sodium PPi. The cell lysates were centrifuged at 16,000 × *g* for 10 min at 4°C, and the resulting supernatant was incubated with antibodies for 2 h at 4°C. Protein A-Sepharose (Amersham Pharmacia) that had been equilibrated with the same solution was added to the mixture, and then the mixture was rotated for 1 h at 4°C. The resin was separated by centrifugation, washed five times with ice-cold lysis buffer, and then boiled in SDS sample buffer. Immunoblot analysis was performed with primary antibodies, horseradish peroxidase–conjugated antibodies to mouse or rabbit IgG (1:10,000 dilution; Promega), and an enhanced chemiluminescence system (Amersham Pharmacia).

Establishment of stable transfectants by using a retrovirus expression system. Complementary DNAs were subcloned into pMX-puro (kindly provided by T. Kitamura, Tokyo University), the resulting vectors were used to transfect Plat A cells, and then recombinant retroviruses were generated (23). LNCaP cells were infected with the recombinant retroviruses and selected in medium containing puromycin (2 μg/mL; Sigma).

RNAi. The pMX-puro II vector in which the U3 portion of the 3′ long terminal repeat was deleted was kindly provided by Dr. T. Kamura (Nagoya University; ref. 24). The hairpin sequences specific for human TRIM68 mRNAs corresponded to nucleotides 329 to 349 (siTRIM68-1) and 796 to 816 (siTRIM68-2) of the respective coding regions. The hairpin sequences specific for enhanced green fluorescent protein (GFP; Clontech) mRNA were used as a control. Recombinant retroviruses were generated and used to infect LNCaP cells as described above. After selection in medium containing puromycin (2 μg/mL), the resulting cell lines were checked by immunoblot analysis with anti-TRIM68 antibody.

Dual-luciferase assay. Cells were seeded in 24-well plates at 1×10^5 per well (LNCaP) or 5×10^4 per well (PC3 and CWR22Rv1) and incubated at 37°C with 5% CO_2 for 24 h. The mouse mammary tumor virus-luciferase (MMTV-Luc) reporter plasmid and the pRL-TK *Renilla* luciferase plasmid (Promega) were transfected with the TRIM68 expression vector into LNCaP and CWR22Rv1 cells or with the AR expression vector into PC3 cells using Fugene HD reagent (Roche). Estrogen-response element reporter plasmid (ERE-Luc) was used for the estrogen receptor (ER)–luciferase assay. Transfected cells were incubated in 10% charcoal-treated FBS (Equitech-Bio) medium for 48 h and then washed and treated with or without 10 nmol/L dihydrotestosterone for 24 h, harvested, and assayed for luciferase activity with a Dual-Luciferase Reporter Assay System (Promega). The luminescence was quantified with a luminometer (Promega).

PSA expression and secretion assays. LNCaP cell lines were seeded in six-well plates and incubated in 10% charcoal-treated FBS medium for 48 h and then washed and treated with or without 10 nmol/L dihydrotestosterone for 24 h. The cells were lysed and subjected to immunoblotting with anti-PSA antibody. Cell culture media were collected and assayed for PSA concentration by ELISA analysis using a TOSOH II PA monoclonal immunoenzyme assay kit.

Cell proliferation assay. LNCaP cell lines were incubated in 10% charcoal-treated FBS medium for 48 h and then plated into 96-well plates at 5,000 per well in 100 μL medium. Cells were treated with 10 nmol/L dihydrotestosterone and refed with fresh medium containing dihydrotestosterone every 2 d. MTS cell proliferation assay was performed using CellTiter 96 one solution (Promega) according to the manufacturer's instructions.

Colony formation assay in soft agar. LNCaP cells were plated at a density of 1×10^4 cells in 60-mm dishes containing 0.4% top low-melting agarose and 0.5% bottom low-melting agarose medium. Colonies with a diameter of >0.1 mm were counted after 3 wk.

Reverse transcription and real-time quantitative PCR. Total RNA (3 μg) isolated from various cell lines, human prostate cancers, and adjacent normal tissues with the use of TRI Reagent (Sigma) was subjected to reverse transcription with MMLV Reverse Transcriptase (Invitrogen). The resulting cDNA was subjected to real-time quantitative PCR by TaqMan gene expression assays (Applied Biosystems) following the manufacturer's instructions. The assays were performed with a TRIM68-specific TaqMan probe and primers (synthesized by Applied Biosystems) in an ABI-PRISM 7000 Sequence Detection System (Applied Biosystems). TATA box-binding protein (TBP) was selected as an internal control to normalize the expression levels. Each sample was tested in triplicate.

Human tissue samples. Tissues from 35 cases of primary prostate cancer were surgically resected by radical prostatectomy. Written informed consent was obtained from each patient before surgery. The excised samples from tumor and adjacent normal tissues were obtained within 1 h after the operation. All excised tissues were immediately placed in liquid nitrogen and stored at −80°C until further analysis. Samples were then manually microdissected from frozen sections on microscope and histologically confirmed to be highly homogeneous cancer tissues by H&E staining of step sections.

Immunohistochemical analysis. Tissues were fixed in 4% formaldehyde for 3 d and then embedded in paraffin. Paraffin-embedded sections (3-μm thick) were mounted on silane-treated slides. After drying overnight at 37°C, paraffin was removed from the sections with xylene, and they were then rehydrated with a graded series of ethanol solutions. The tissues were then subjected to immunohistochemical staining with an antibody to TRIM68 (5 μg/mL) by a streptavidin-biotin immunoperoxidase method using an immunohistochemical detection kit (Vectastain Elite; Vector) and diaminobenzidine as a chromogen (Wako) according to the manufacturer's instructions. Immunoreactivity was semiquantitatively classified. Two independent investigators reviewed and scored slides observed under a microscope by categorizing staining intensity of characteristic staining cells as negative, weak, medium, or strong (scored as 0–3). The final score was

obtained by multiplying the percentage of positive cells by the intensity score with an estimated score range of 0 to 300.

Statistical analysis. We used the unpaired Student's *t* test and the Mann-Whitney *U* test to determine statistical significance of experimental data.

Results

TRIM68 has a ubiquitin ligase activity and is predominantly expressed in the prostate cancer cell line LNCaP. TRIM68 has a RING finger domain at its NH_2 terminus and belongs to the TRIM family of proteins, some of which have been reported to be E3 ubiquitin ligases (18). To determine whether TRIM68 actually mediates an E3 ligase activity, we generated recombinant TRIM68 protein by using a baculovirus expression system and performed an *in vitro* ubiquitination assays with various combinations. Immunoblot analysis using an anti-ubiquitin antibody revealed that TRIM68 exhibits ubiquitination activity only in the presence of E1, E2 (Ubc4), ubiquitin, ATP, and TRIM68 (Fig. 1*A*, *top*). The lack of any of these components prevented autoubiquitination of TRIM68. In addition, an *in vitro* ubiquitination assay using anti-TRIM68 antibody showed that TRIM68 has an autoubiquitination activity (Fig. 1*A*, *bottom*). These findings indicate that TRIM68 is a bona fide E3 ligase. To further investigate the region of TRIM68 responsible for ubiquitination, we generated a deletion mutant lacking a RING finger domain (ΔRING) of TRIM68 and then performed an *in vitro* ubiquitination assay (Fig. 1*B*). The *in vitro* ubiquitination assay showed that the deletion mutant has no E3 ligase activity, indicating that the RING finger domain is indispensable for E3 ubiquitin ligase activity of TRIM68.

To study the expression profile of TRIM68, we measured TRIM68 mRNA levels in various human cell lines of different origins by using real-time quantitative reverse transcription–PCR (RT-PCR). The gene expression of TRIM68 was found predominantly in the prostate cancer cell line LNCaP compared with its expression in other cell lines, including the prostate cancer cell lines CWR22Rv1 and PC3, B-cell lymphoma cell line Namalwa, embryonic kidney cell line 293, breast cancer cell lines T47D and MCF7, uterine epithelial carcinoma cell line HeLa, neuroblastoma cell line SH-SY5Y, and hepatocellular carcinoma cell line HepG2 (Fig. 1*C*). Next, we compared the protein levels of TRIM68 by immunoblotting in hormone-related cancer cell lines, including LNCaP, 22Rv1, PC3, T47D, and MCF7. Consistent with the observed mRNA expression pattern, TRIM68 protein was found to be abundantly expressed in the prostate cancer cell line LNCaP compared with its expression in other cell lines (Fig. 1*D*).

Interaction between TRIM68 and AR. Given that TRIM68 is highly expressed in the androgen-responsive prostate cancer cell line LNCaP, we hypothesized that TRIM68 is associated with prostate cancer and particularly the AR signaling pathway. To test the possibility, we verified interaction between endogenous TRIM68 and AR in LNCaP cells by immunoprecipitation using antibodies to TRIM68 and AR (Fig. 2*A*). Furthermore, to determine the domain of AR that interacts with TRIM68, deletion mutants of AR were constructed for *in vivo* binding assays (Fig. 2*B*). HA-tagged AR mutants and FLAG-tagged TRIM68 were expressed in HEK293T cells, and the cell lysates were subjected to immunoprecipitation with anti-FLAG antibody. The results showed that AR-L, including the ligand-binding domain, was coprecipitated with TRIM68 but AR-ND, including the amino-terminal domain and DNA-binding domain, was not, suggesting that the ligand-binding domain is responsible for interaction with TRIM68 (Fig. 2*C*).

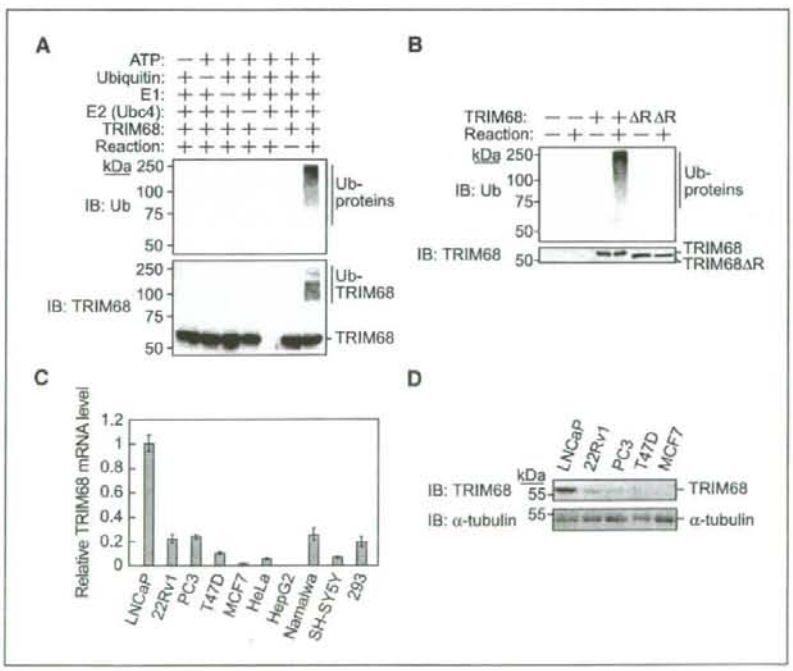

Figure 1. Ubiquitin ligase TRIM68 is predominantly expressed in prostate cancer LNCaP cells. *A*, ATP-dependent, E1-dependent, and E2-dependent ubiquitin ligase activity of TRIM68. An *in vitro* ubiquitination assay was performed with the indicated combinations of ATP, ubiquitin, E1, E2 (Ubc4), and TRIM68. The reaction mixtures were also subjected to immunoblot analysis with antibodies to ubiquitin (*top*) and TRIM68 (*bottom*). *B*, RING finger domain is indispensable for ubiquitin ligase activity of TRIM68. An *in vitro* ubiquitination assay was performed with equimolar amounts of TRIM68 derivatives (TRIM68 and TRIM68ΔR) in the presence of ATP, E1, and E2 (Ubc4). The reaction mixtures were also subjected to immunoblot analysis with antibodies to ubiquitin (*top*) and TRIM68 (*bottom*). *C*, quantitative analysis of TRIM68 transcript in various cell lines. TRIM68 mRNA expression levels in various human cell lines of different origins were quantified by real-time quantitative RT-PCR. The expression level of TRIM68 mRNA was normalized to that of TBP mRNA. The expression level of TRIM68 mRNA in LNCaP cells was defined as 1. *Columns*, mean of values from three independent experiments; *bars*, SD. *D*, TRIM68 protein expression in sex hormone–related cancer cell lines. Cell lysates from prostate or breast cancer cell lines were subjected to immunoblot analysis with anti-TRIM68 and anti–α-tubulin antibodies. Prostate cancer cell lines: LNCaP, 22Rv1, and PC3; breast cancer cell lines: T47D and MCF7.

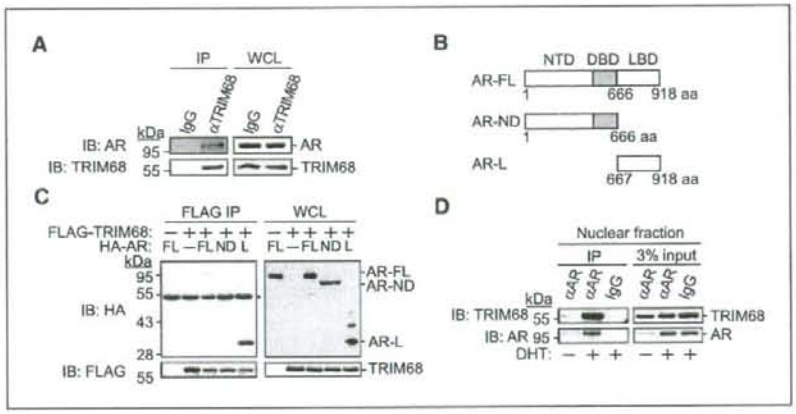

Figure 2. Interaction between TRIM68 and AR. *A*, interaction between endogenous TRIM68 and AR in prostate cancer cells. LNCaP cells were lysed and subjected to immunoprecipitation with anti-TRIM68 antibody followed by immunoblotting with anti-AR and anti-TRIM68 antibodies. Irrelevant IgG was used as a control. Cell lysates (WCL) were also subjected to immunoblotting to confirm the expression levels of endogenous TRIM68 and AR. *B*, schematic representation of the domain structures of AR derivatives. Deletion mutants of AR were constructed. AR-FL has full-length AR. AR-ND has an amino-terminal domain plus DNA-binding/hinge domain of AR. AR-L has a ligand-binding domain of AR. *NTD*, amino-terminal domain; *DBD*, DNA-binding/hinge domain; *LBD*, ligand-binding domain. *C*, ligand-binding domain of AR is responsible for the interaction with TRIM68. Expression vectors encoding HA-tagged AR derivatives (AR-FL, AR-ND, and AR-L) and FLAG-tagged TRIM68 were transfected into HEK293T cells as indicated. After 48 h, cells were lysed and subjected to immunoprecipitation with anti-FLAG antibody followed by immunoblotting with anti-HA and anti-FLAG antibodies. Whole-cell lysates were also subjected to immunoblotting to confirm the expression of AR derivatives and TRIM68. *, IgG heavy chain. *D*, interaction of TRIM68 with AR in the nucleus is enhanced by dihydrotestosterone (*DHT*) treatment. LNCaP cells were incubated in 10% charcoal–treated FBS medium for 48 h and then treated with or without 10 nmol/L dihydrotestosterone for 24 h. Subcellular fractions were separated biochemically, and then nuclear fractions were immunoprecipitated with anti-AR antibody followed by immunoblotting with anti-TRIM68 and anti-AR antibodies. Irrelevant IgG was used as a control. A portion of the nuclear extracts corresponding to 3% of the input for immunoprecipitation was also subjected to immunoblotting to confirm the expression levels of endogenous TRIM68 and AR in the nucleus.

Next, to confirm subcellular colocalization of TRIM68 and AR in the nucleus, we performed an immunoprecipitation assay using nuclear fractions of LNCaP cells treated or not treated with dihydrotestosterone. The immunoprecipitation assay showed that the nuclear interaction of TRIM68 with AR was enhanced by dihydrotestosterone treatment, suggesting that TRIM68 serves as a coregulator for androgen-dependent transcription (Fig. 2*D*).

TRIM68 enhances AR-mediated transcriptional activity. Having shown coprecipitation and colocalization of TRIM68 and AR, we next examined whether TRIM68 functionally affects AR-mediated transcription. To examine the effect of TRIM68 on AR-mediated transcriptional activity, we performed a luciferase reporter assay using an MMTV promoter-driven luciferase construct (MMTV-Luc). A TRIM68 expression vector and MMTV-Luc were transfected into LNCaP and CWR22Rv1 cells, and luciferase assays were then performed with and without dihydrotestosterone. The luciferase assays showed that TRIM68 enhances androgen-dependent AR-mediated transcriptional activity in a dose-dependent manner, whereas TRIM68ΔRING mutant, which lacks ubiquitin ligase activity, showed a dominant negative effect, suggesting that TRIM68 acts as a positive regulator for AR signaling and that ubiquitin ligase activity of TRIM68 is indispensable for AR transactivation (Fig. 3*A*).

To confirm the physiologic role of TRIM68 in AR-mediated transcription, we used RNAi to knockdown endogenous TRIM68 in LNCaP cells. Two different short interference RNAs (siRNA) targeting TRIM68 were introduced into LNCaP cells by using a retroviral infection system. RNAi treatment resulted in significant silencing of TRIM68 at protein level in LNCaP cells (Fig. 3*B*, *left*). To examine the effect of the depletion of TRIM68 on AR-mediated transcription, we performed a relative luciferase assay for AR signal in LNCaP cells transfected with TRIM68 siRNA. The relative luciferase activities of cells transfected with TRIM68 siRNA were decreased compared with those of cells transfected with the control siRNA (Fig. 3*B*, *right*).

To determine whether the effect of TRIM68 is specific to AR-mediated transcription, we transfected expression vectors encoding TRIM68 and wild-type AR, glucocorticoid receptor (GR) or ER into the androgen-independent prostate cancer cell line PC3 and performed luciferase reporter assays using each reporter system for AR, GR, and ER. Luciferase assays showed that TRIM68 markedly enhances AR-mediated transcription in PC3 cells transfected with AR, whereas TRIM68 enhances GR-mediated transcription to a lesser degree and has no effect on ER-mediated transcription (Fig. 3*C*). These findings indicate that TRIM68 is a comparatively specific coactivator for AR.

It has been reported that ubiquitin modification of substrates and the sequential degradation by the proteasome is involved in transcription activity of AR (25). To determine whether proteasome activity is required for TRIM68-mediated transcriptional activity of AR, we performed a luciferase assay for AR transactivation in the presence or absence of a proteasome inhibitor, MG132. TRIM68 enhanced AR transactivation in the absence of MG132, whereas the effect of TRIM68 was dramatically suppressed in the presence of MG132, indicating that the proteasome activity is required for the effect of TRIM68 on AR transcriptional activity (Fig. 3*D*).

TRIM68 cooperates with TIP60 and p300 to enhance AR-mediated transcriptional activity. The activity of AR is regulated by several posttranslational modifications. Previous studies have shown that AR and coregulators are regulated by histone acetyltransferases, such as TIP60 and p300, to enhance AR transcriptional activity (9, 26). Therefore, we hypothesized that TRIM68 physically or functionally interacts with TIP60. To determine whether TRIM68 physically interacts with TIP60, expression